

Presented by:

Ana Sofía Marulanda-Duque
Estudiante MSc. en Física (Universidad de Antioquia)

Supervised by:

Viviana Rosero (Caltech)
Joshua Marvil (NRAO)

SEARCHING FOR EVIDENCE OF ACCRETION TO MASSIVE PROTOSTARS BEYOND THE CLASSICAL FEEDBACK LIMIT

In Collaboration with:

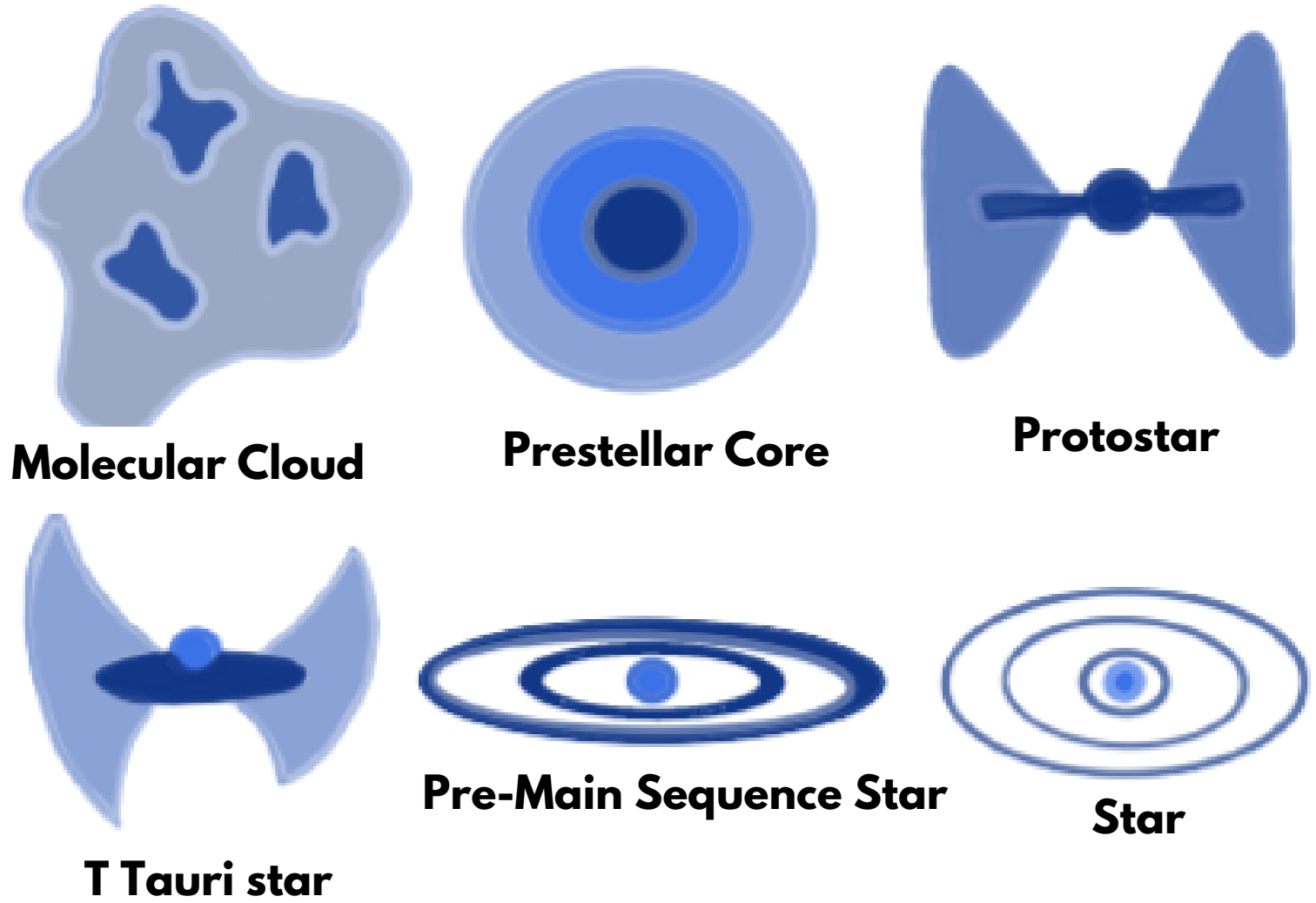
Kei Tanaka (Tokio Tech)
Yichen Zhang (University of Virginia)
Germán Chaparro (Universidad de Antioquia)

November, 2024



Instituto de Física - Universidad de Antioquia

Stellar formation process



1

Low mass systems



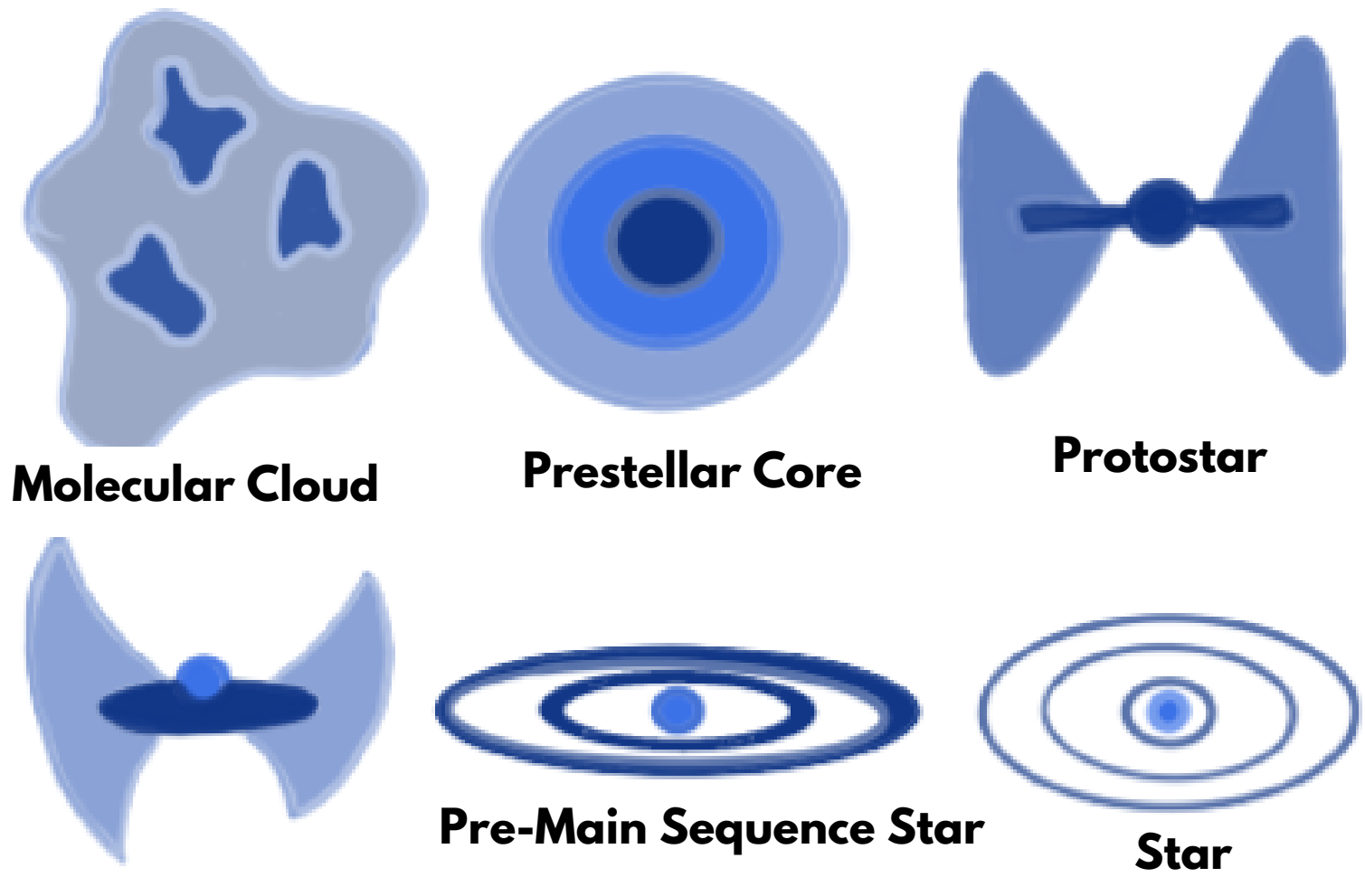
Grupo de
Física y Astrofísica
Computacional
Instituto de Física - Universidad de Antioquia

1

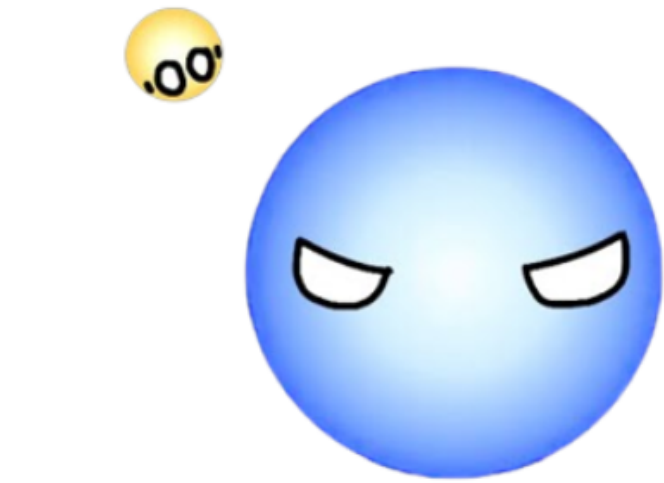
Presented by: Ana Sofía Marulanda-Duque
sofia.marulanda2@udea.edu.co

Stellar formation process

Type B and O stars form, we observe them, but how?



Low mass systems



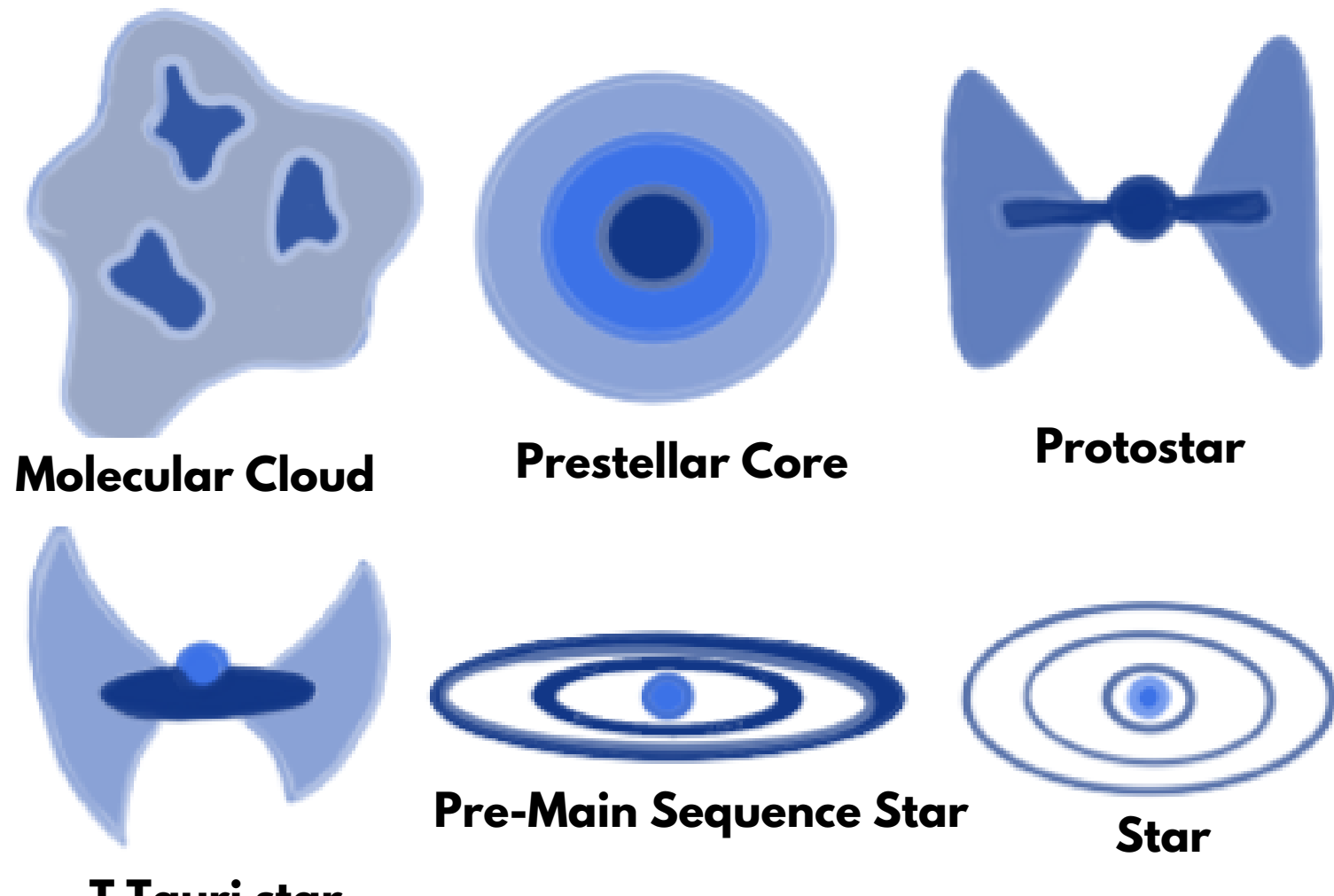
Accretion vs Radiative Feedback problem!

$$M \geq 40 M_{\odot}$$

$$\text{Accretion Rates} > 3 \times 10^{-3} M_{\odot} \text{ yr}^{-1}$$

$$R > 100 R_{\odot}$$

Stellar formation process



Type B and O stars form, we observe them, but how?

Core accretion

Competitive accretion

Protostellar collisions

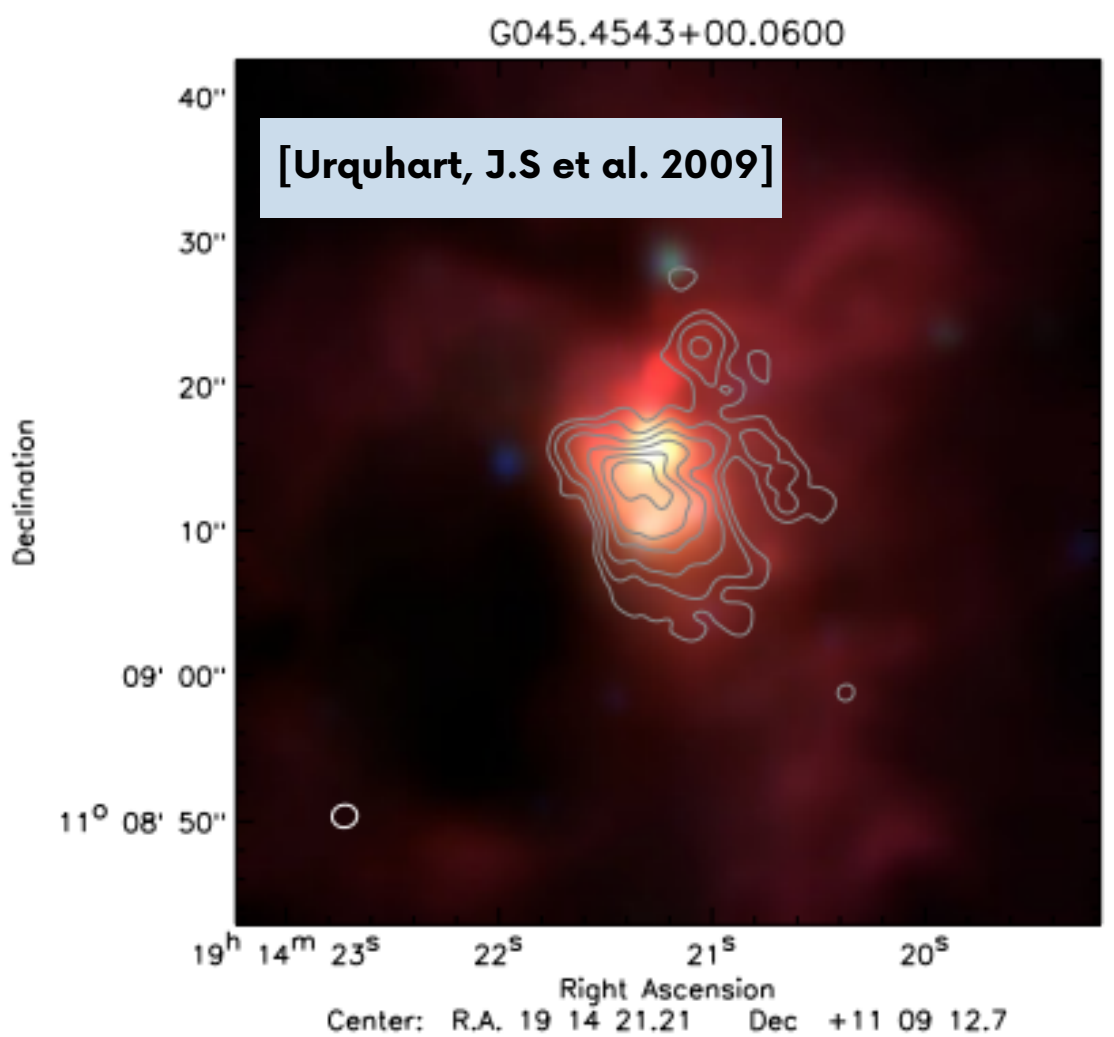


Accretion vs Radiative Feedback problem!

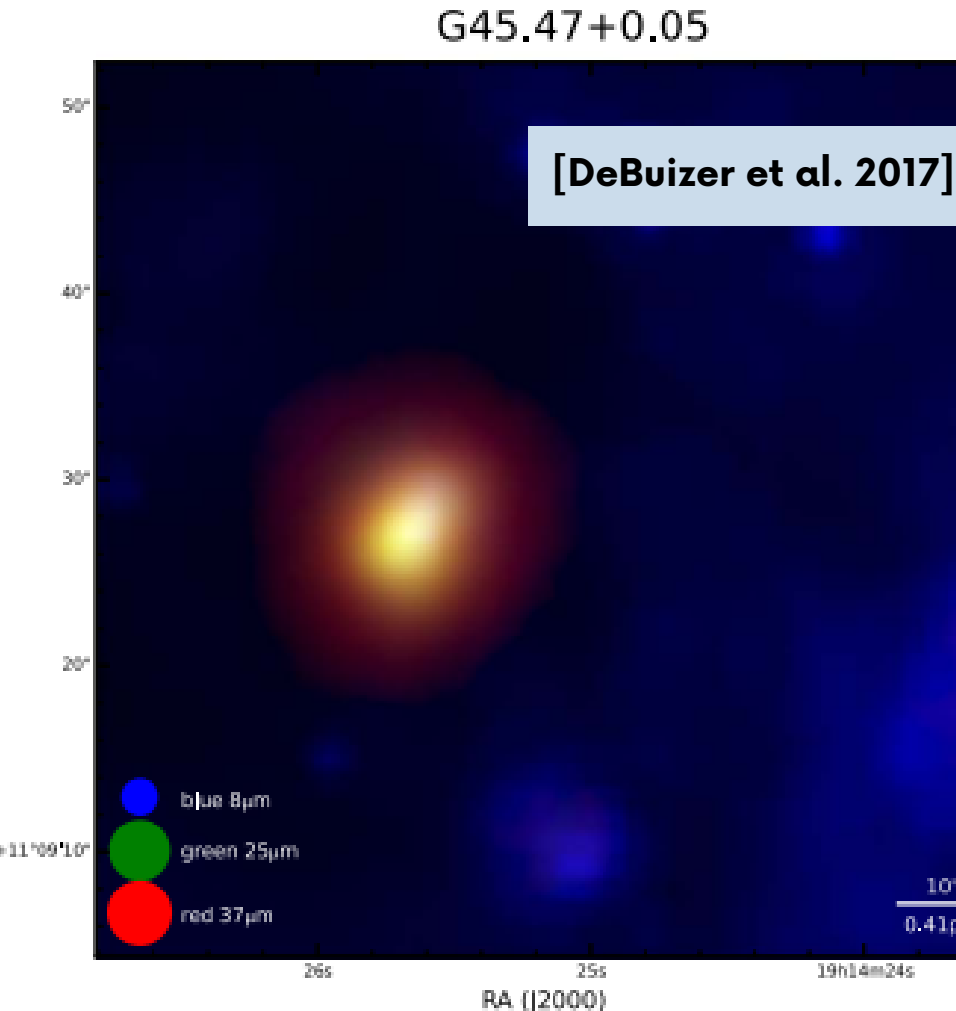
No direct observational evidence so far!

Low mass systems

Observing massive sources is difficult!

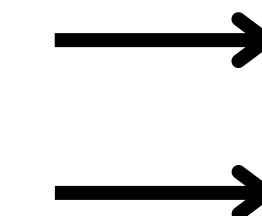


GLIMPSE Spitzer IR in 3.6, 4.5 and 8.0 μm bands (blue, green and red) overlaid with contours of the 6cm radio emission

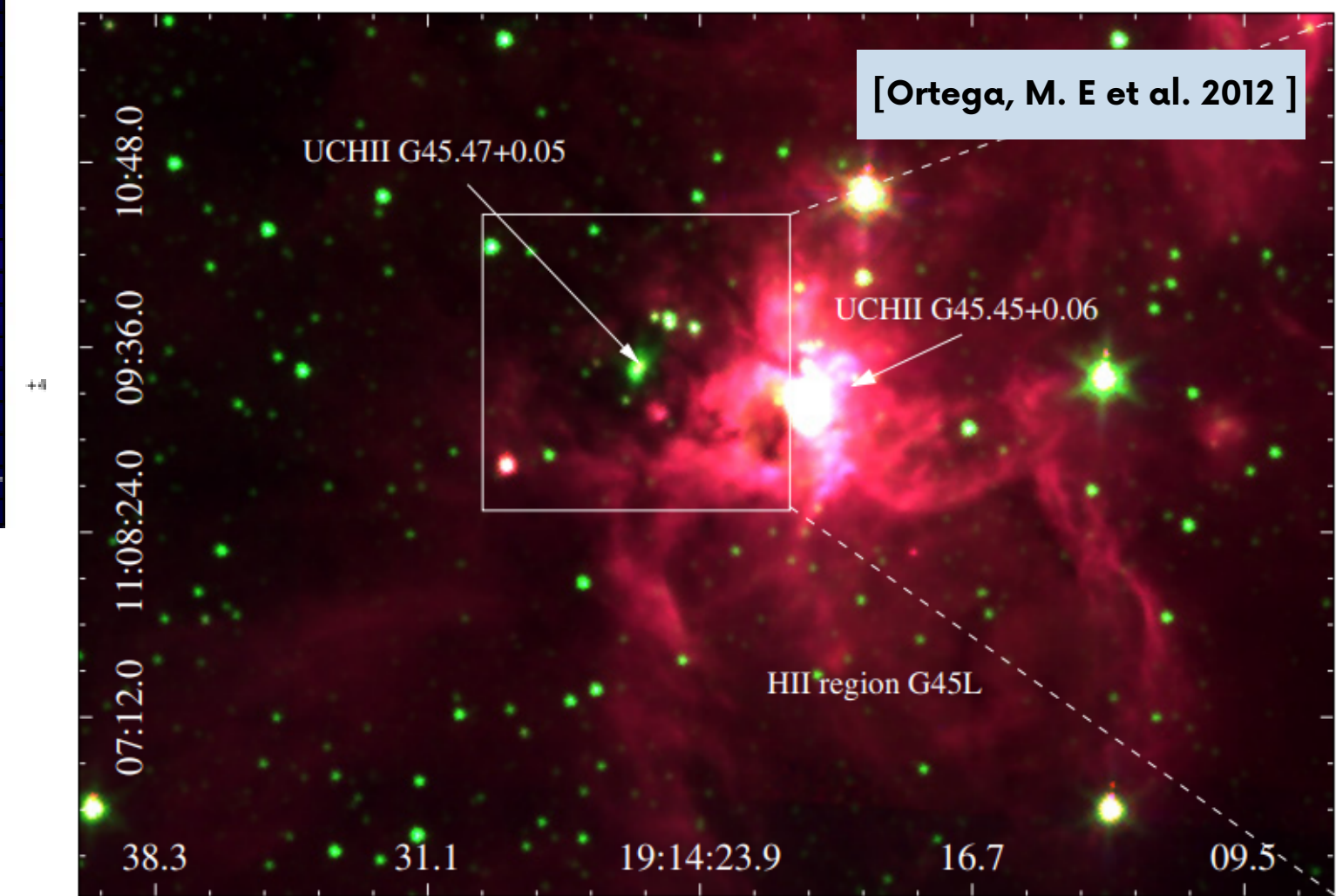


RGB images IR Spitzer

Started being associated with a UCHII region
H₂O and HO masers

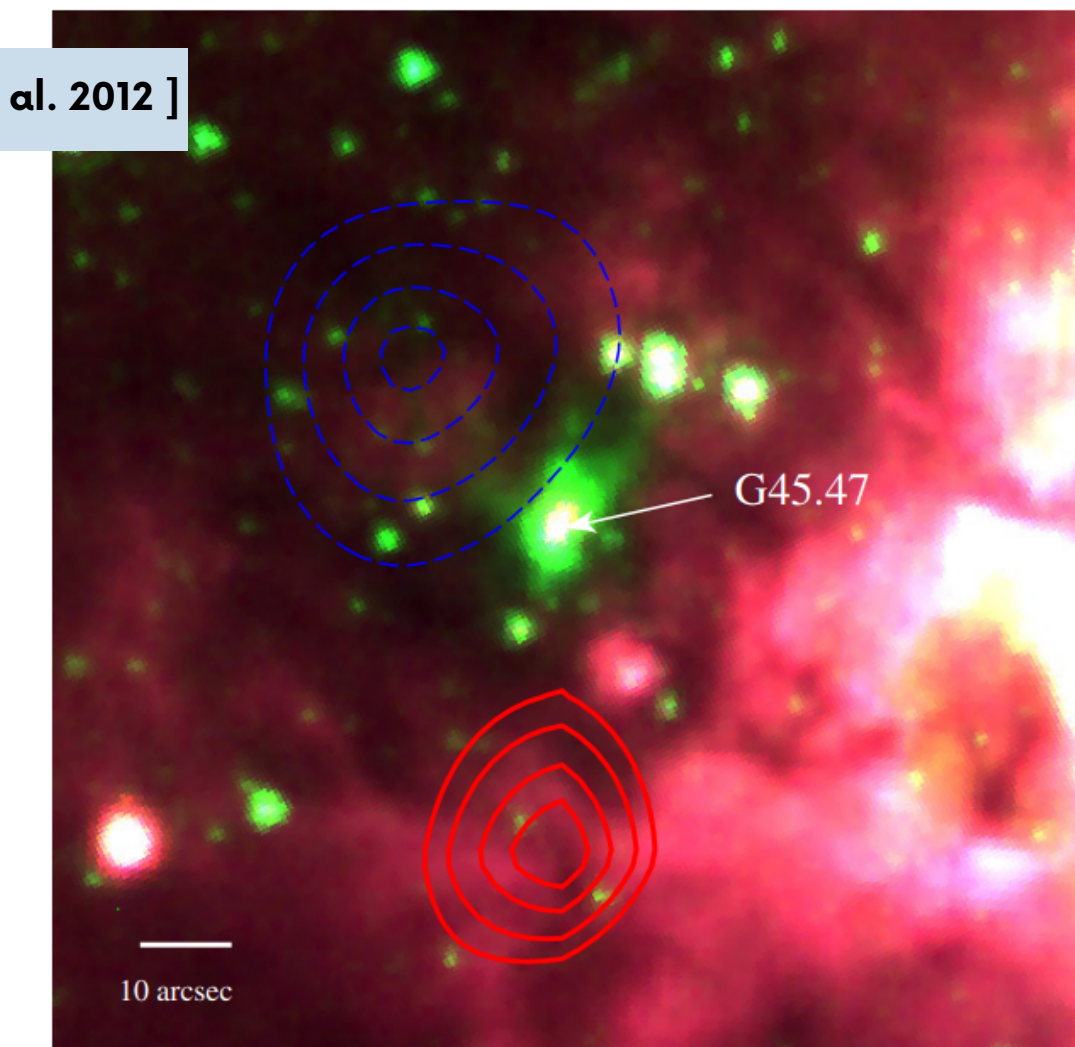
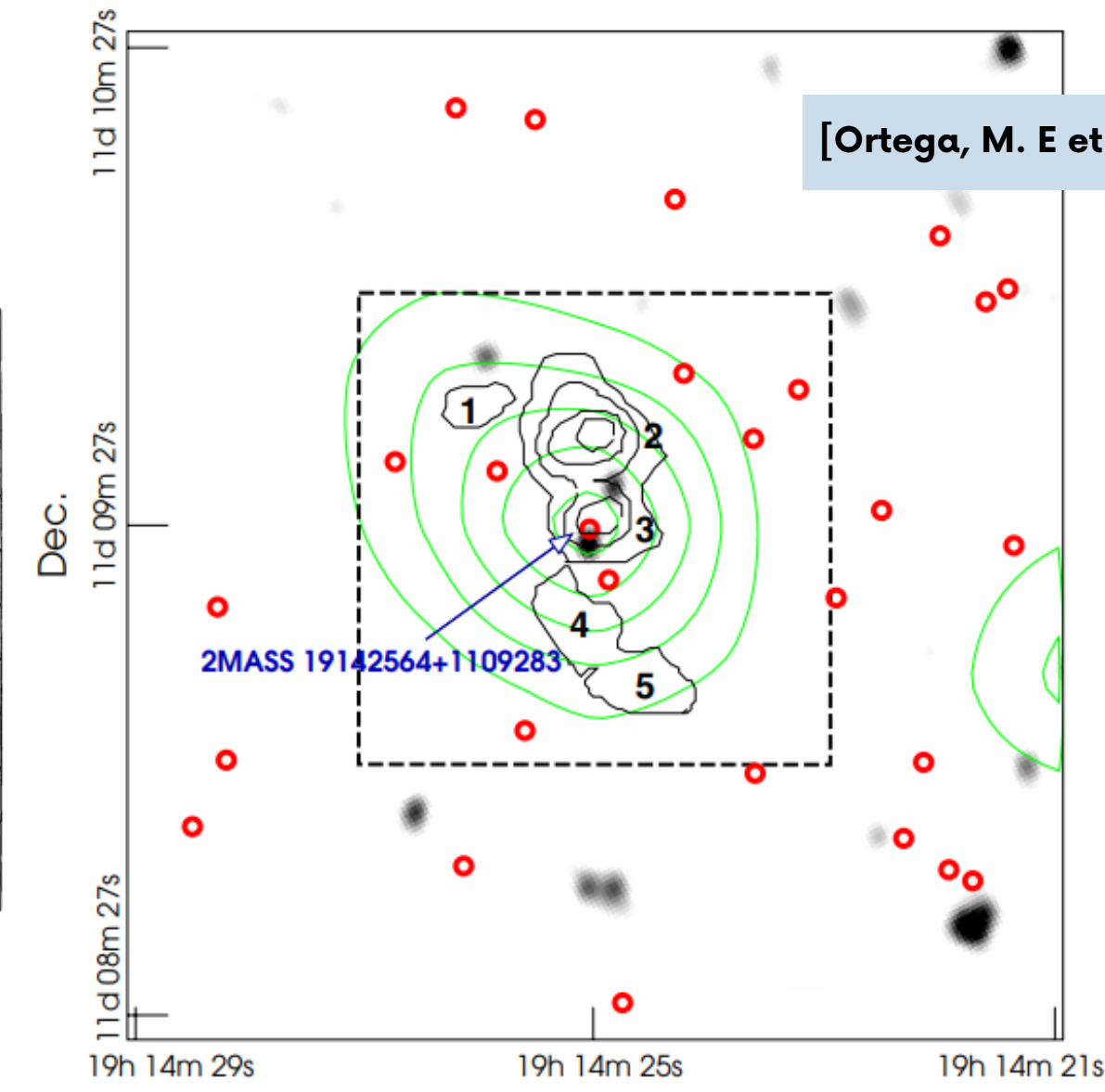
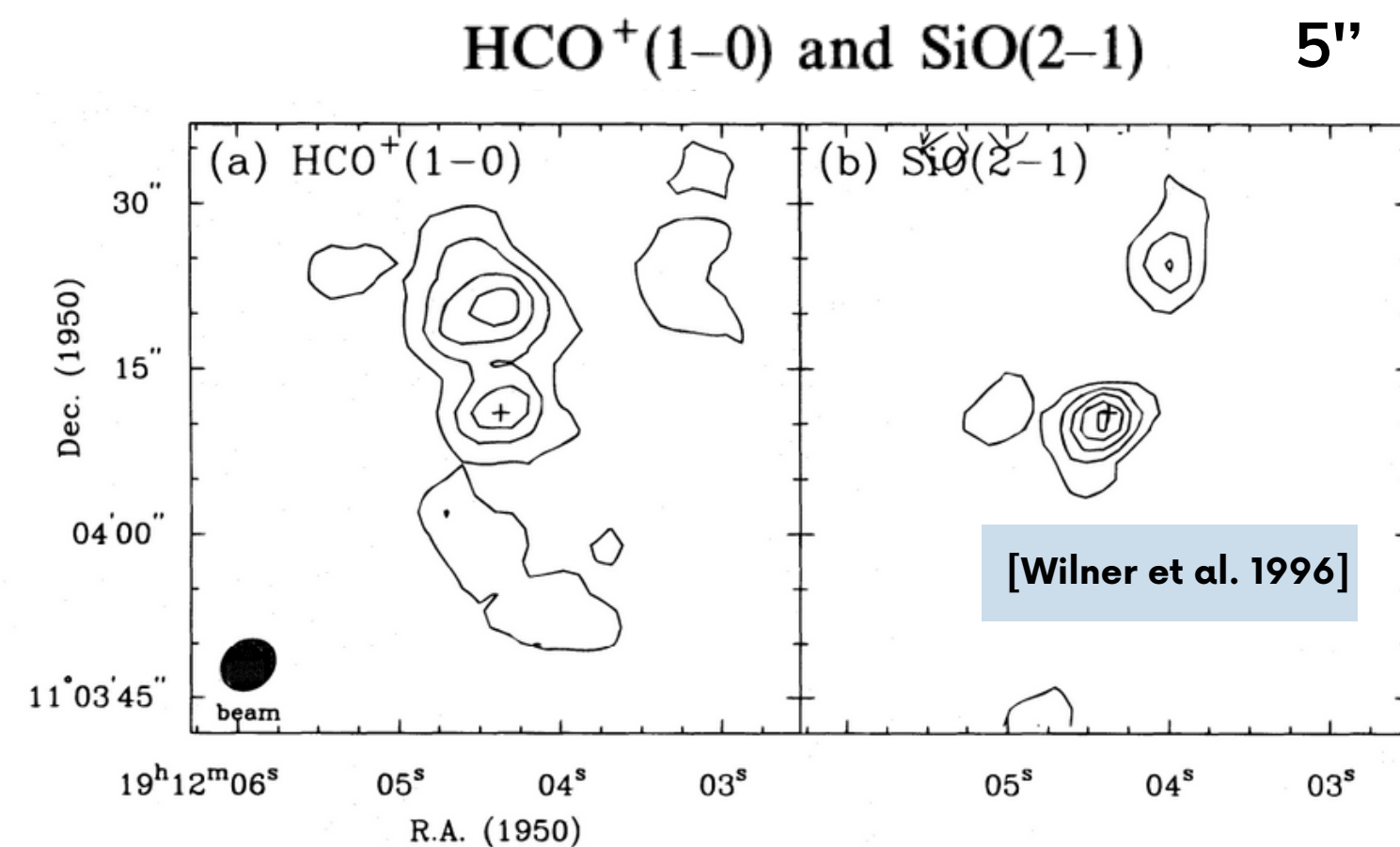


- Wilner et al. 1996
- Wood & Churchwell 1989
- Forster & Caswell 1989



Large scale structure

Searching for infall signatures on the source



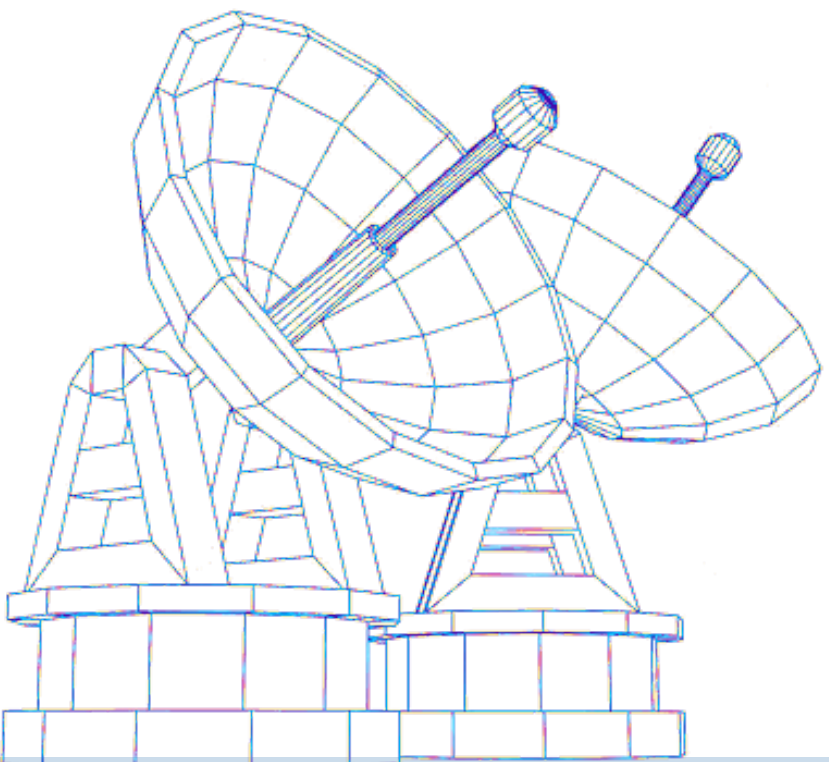
Unable to observe an inverse P Cygni profile that indicates infall of material

Green contours are HCO+ J= 4-3
Radio continuum at 6 cm mapped using ASTE
1-5 HCO+ J= 1-0 clumps region is highly fragmented and consists of dense pockets of gas

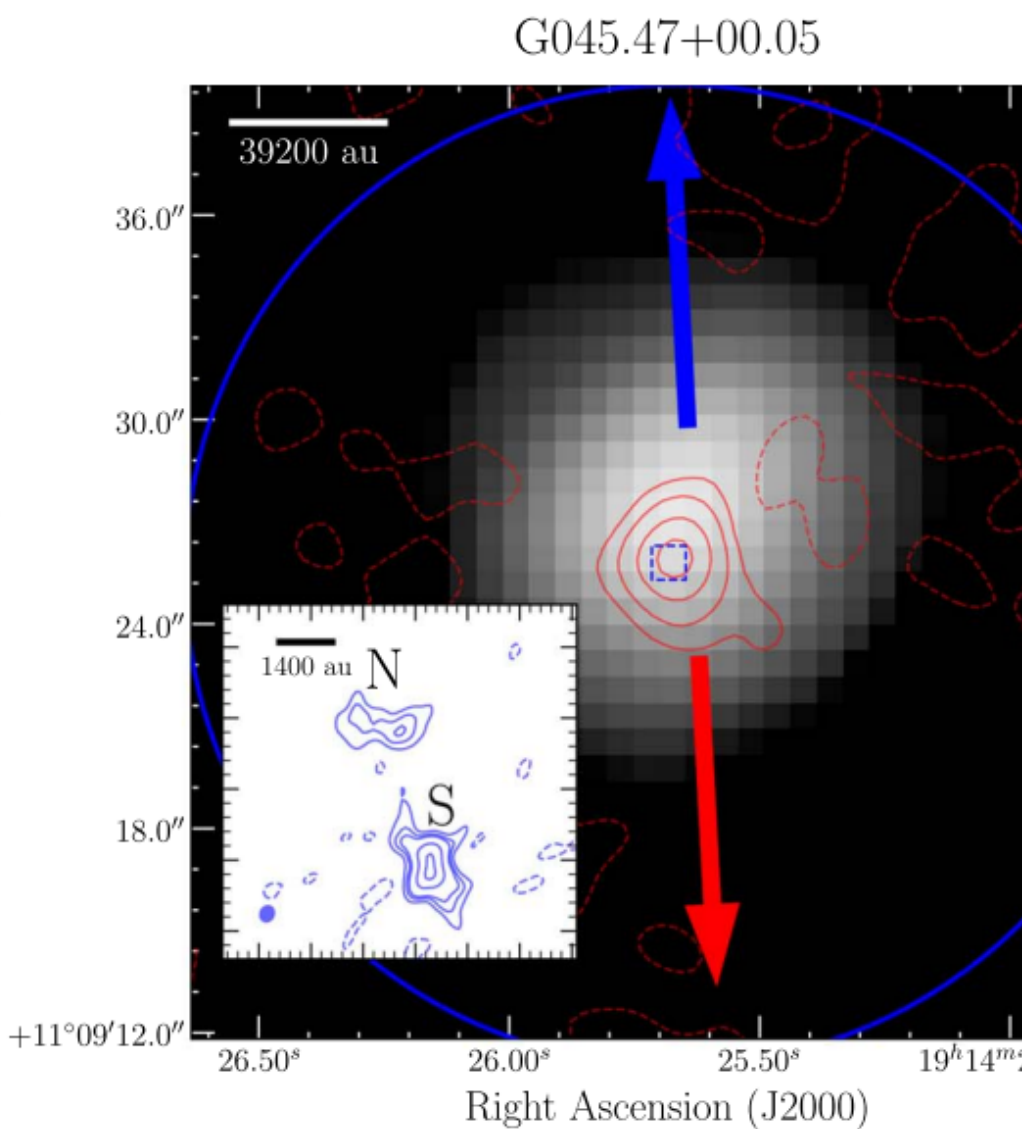
CS J = 7–6 transition reveals the presence of warm and dense gas

Improved sensitivity

The SOFIA Massive (SOMA) Star Formation Surveys

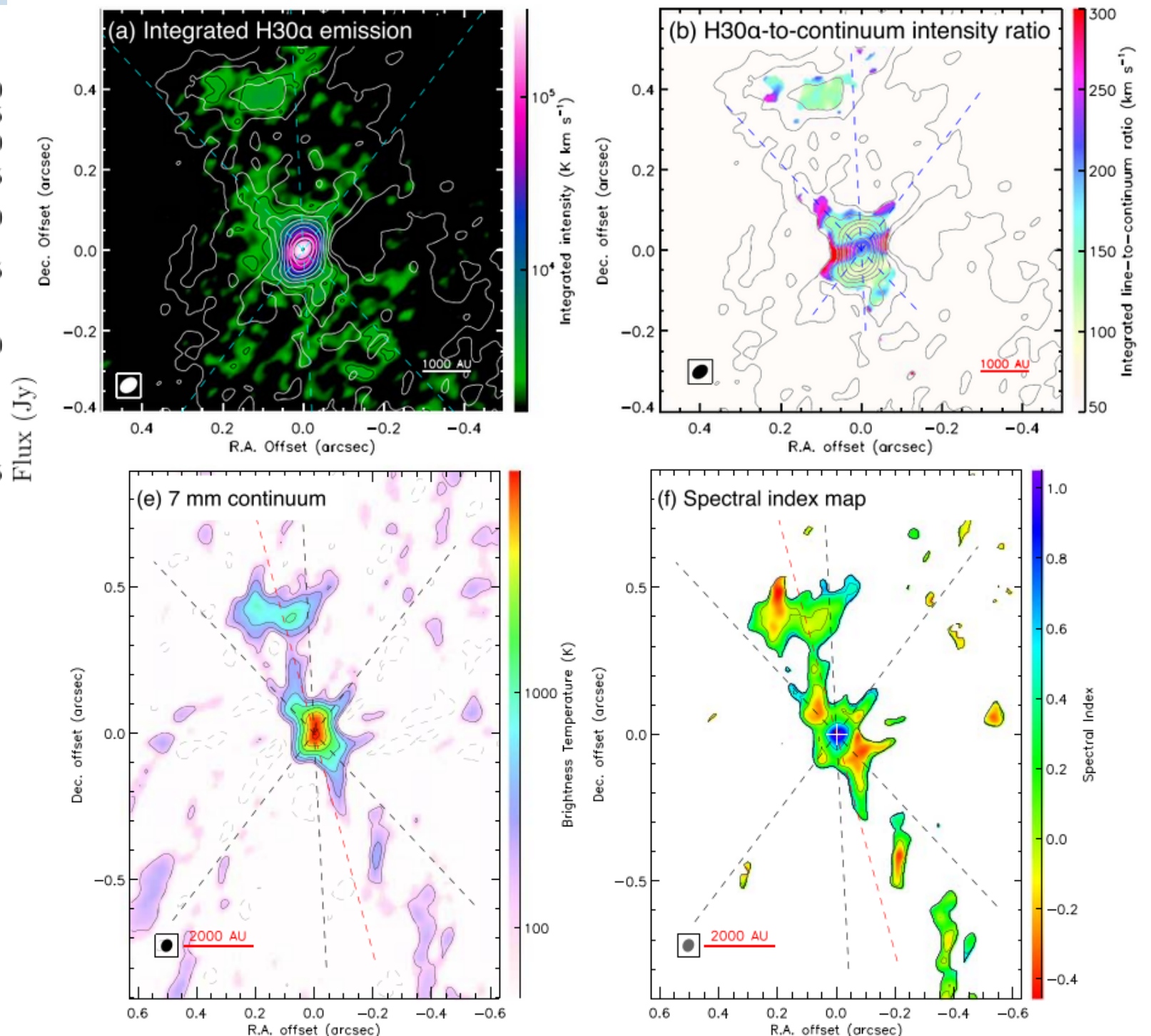


Declination (J2000)



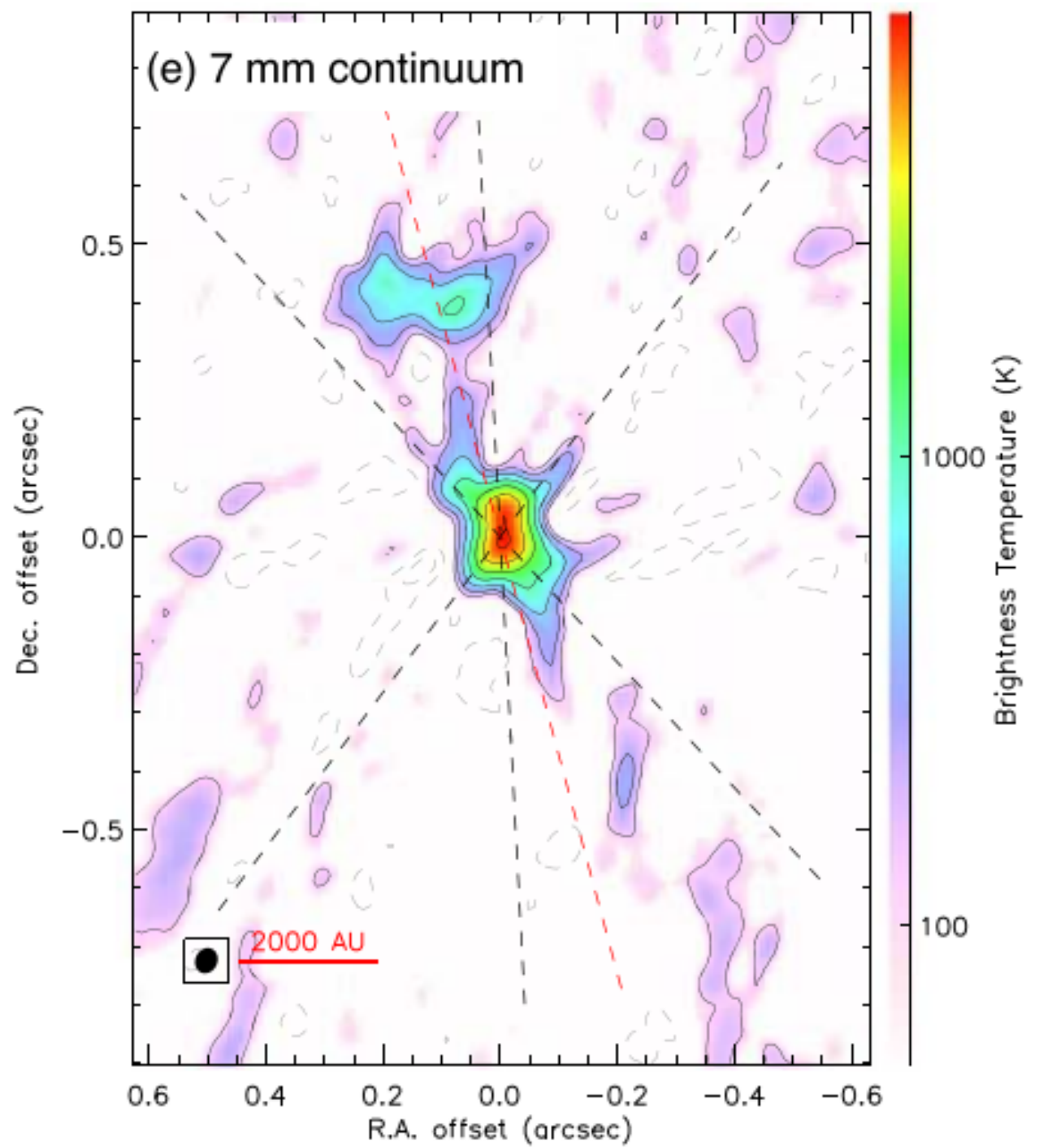
[Rosero, V et al 2019]

[Zhang, Y et al 2019]



G45.47+0.05

[Zhang, Y et al 2019]



Observed with

Alma Band6 / VLA BandQ

Mass

$50M_{\odot}$

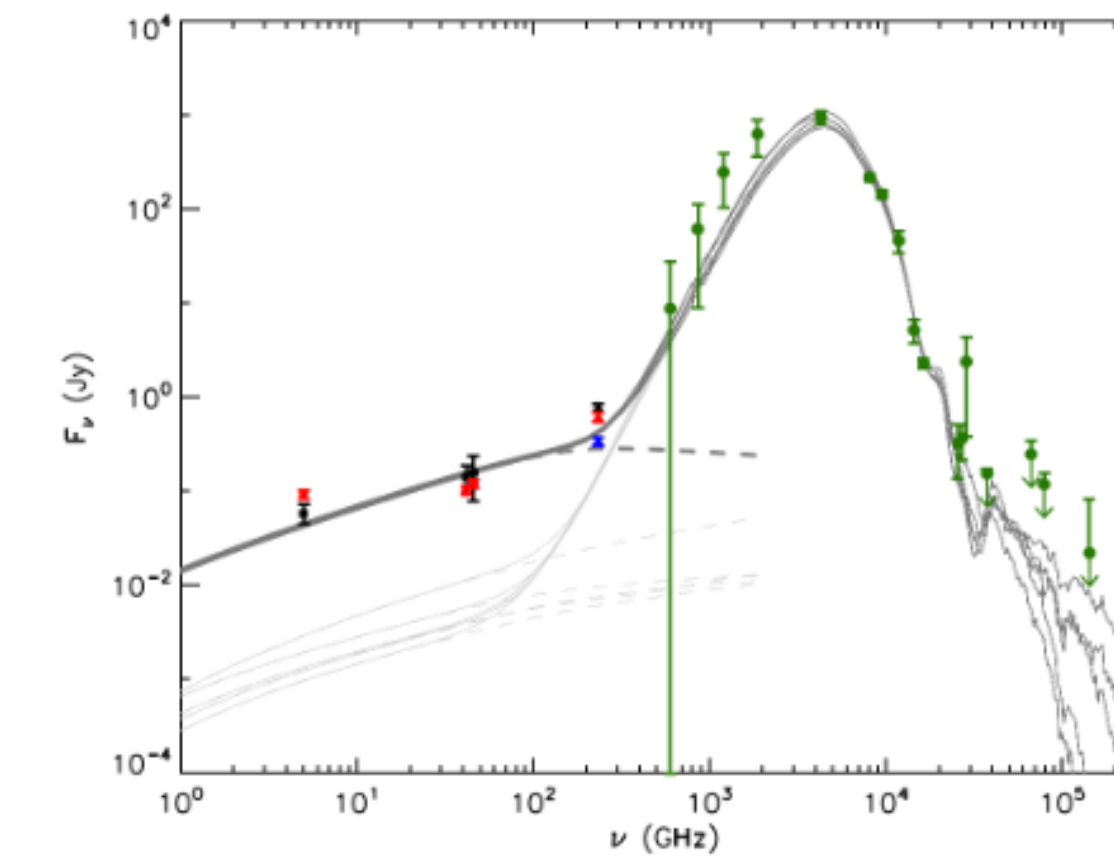
Distance

8.4 kpc

Birth Region

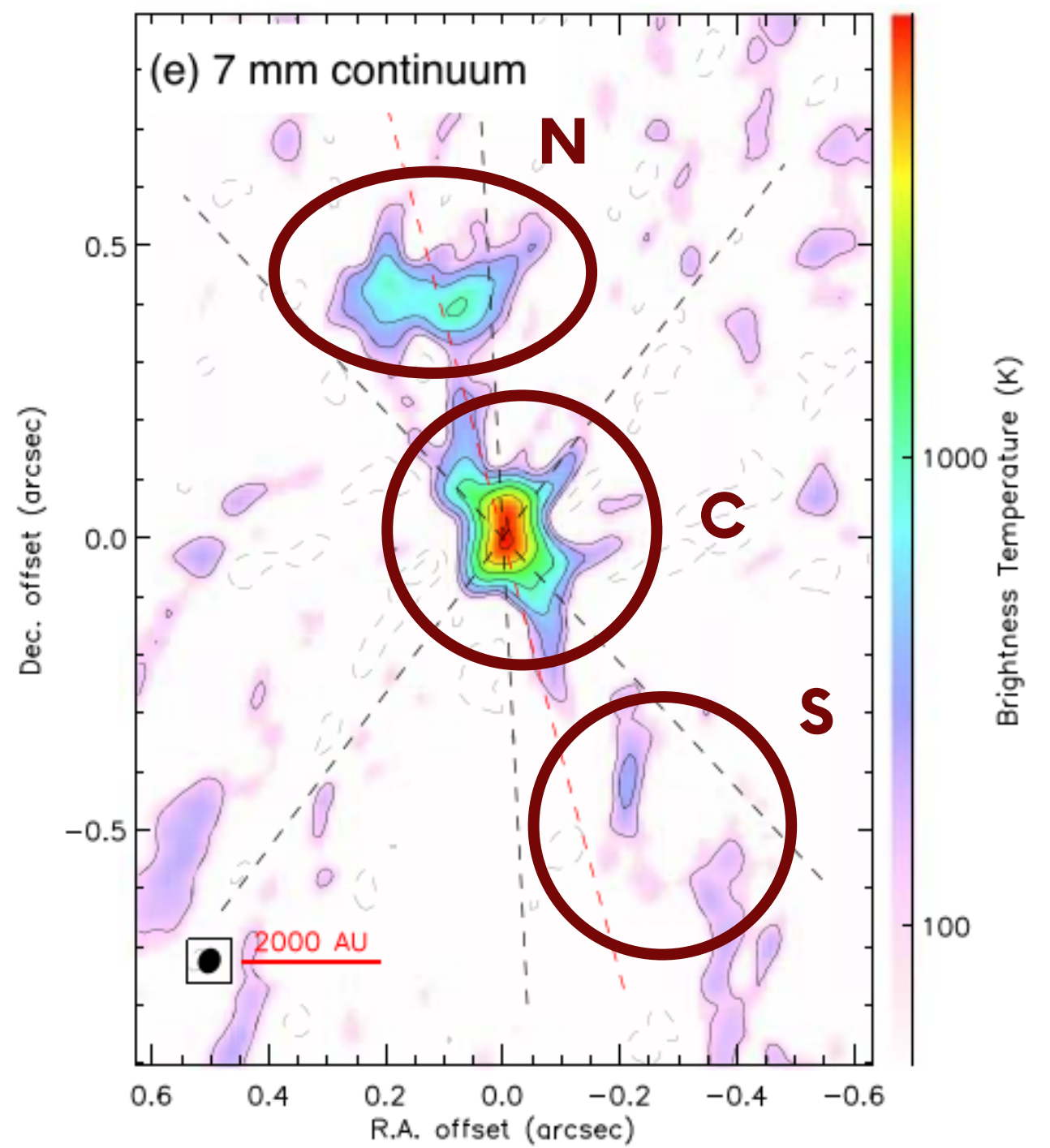
UHCII

Spectral Energy Distribution



G45.47+0.05

[Zhang, Y et al 2019]



Observed with

Alma Band6 / VLA BandQ

Mass

$50M_{\odot}$

Distance

8.4 kpc

Birth Region

UHCII

Disk confirmed through kinematics

Photoionised bipolar outflow

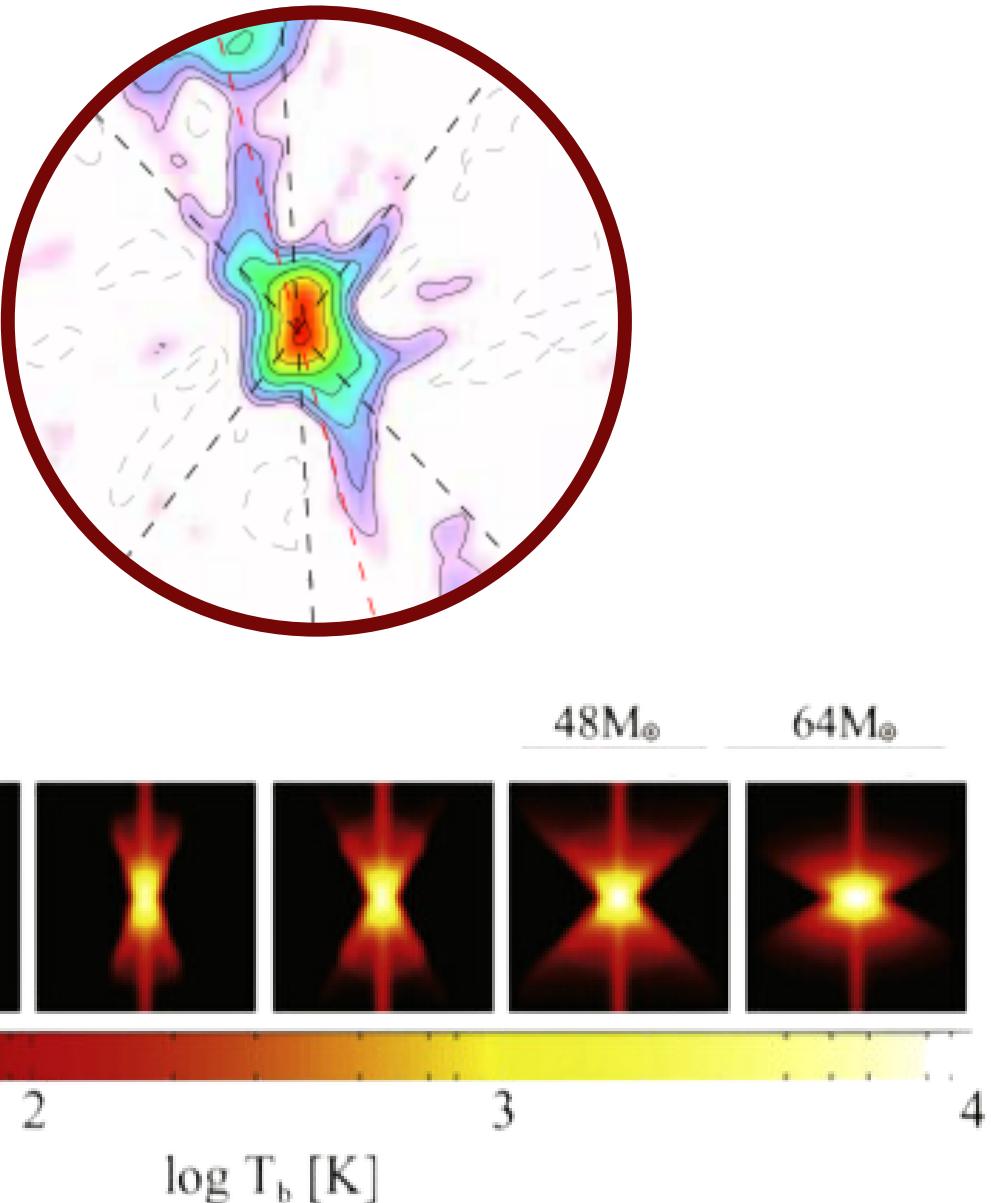
Spectral index
 $\alpha > 0$ Dominant free-free emission
 Some regions $\alpha < -0.5$ indicate non-thermal emission

Inside the ionized outflow: Non-thermal jet candidate

G45.47+0.05

Why is it so special?

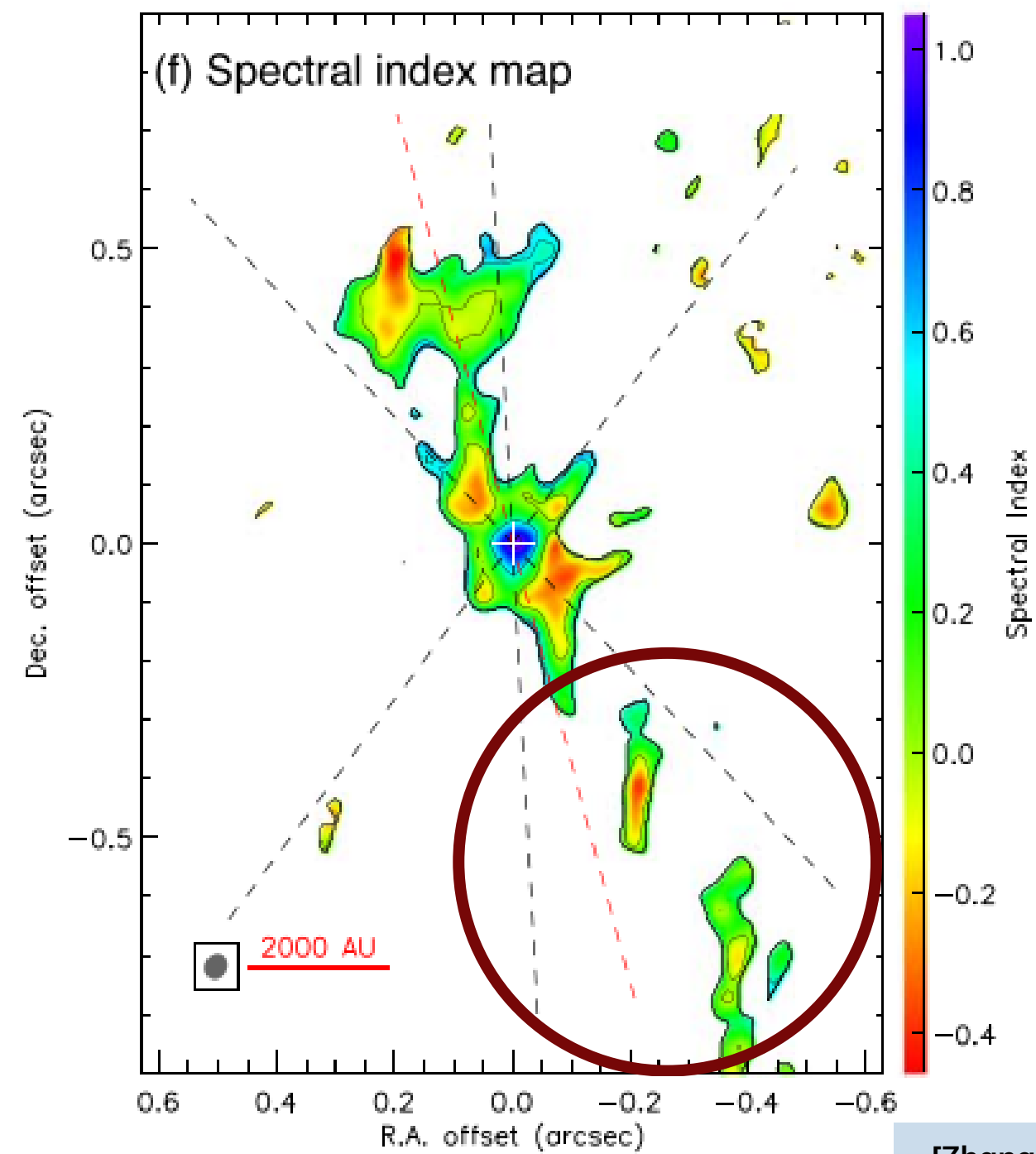
Morphologically, it coincides well with the model



[Tanaka, K.E.I., Tan, J.C., Zhang, Y., 2016]

G45.47+0.05

Very challenging source!



Observed with

Alma Band6 / VLA BandQ

Mass

$50M_{\odot}$

Distance

8.4 kpc

Birth Region

UHCII

Disk confirmed through kinematics

Photoionised bipolar outflow

Spectral index

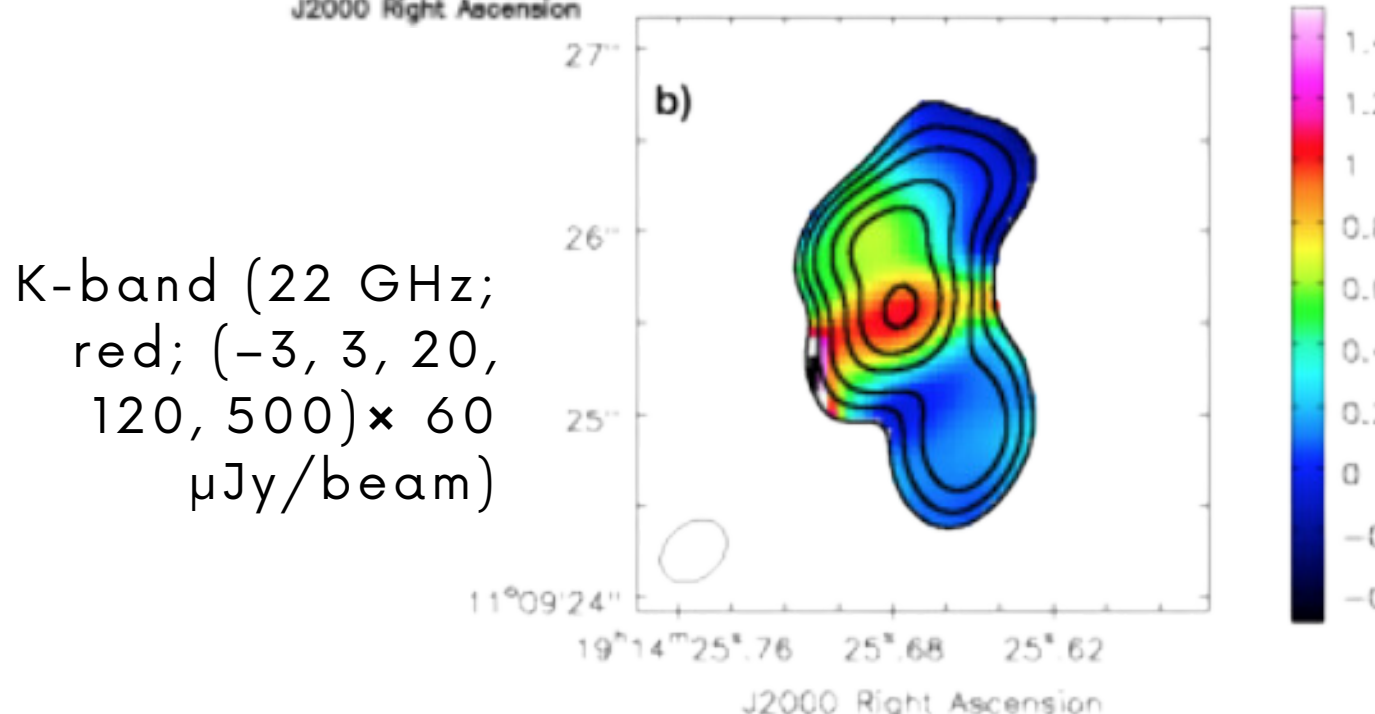
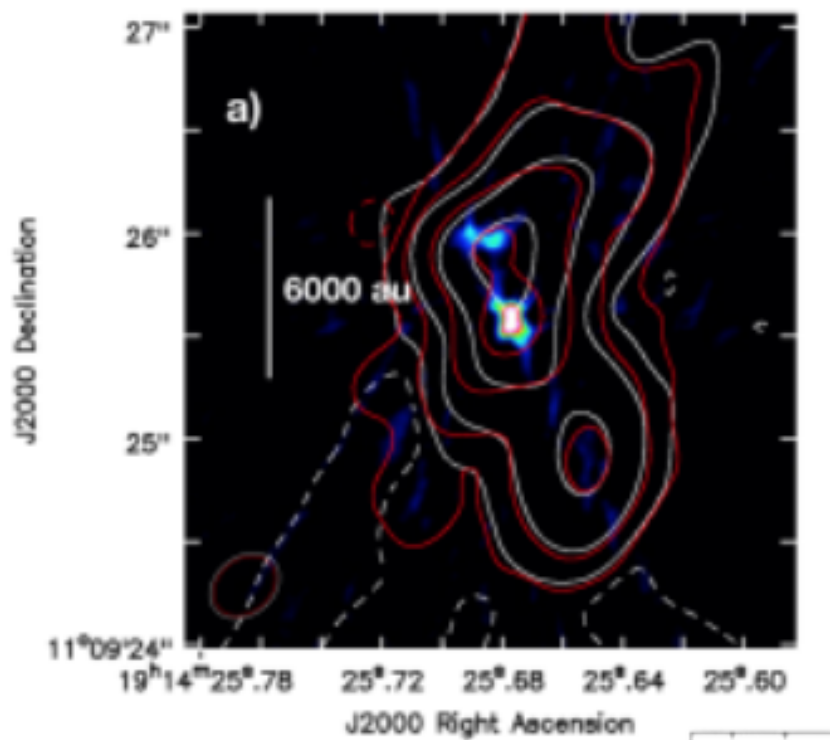
$\alpha > 0$ Dominant free-free emission

Some regions $\alpha < -0.5$ indicate non-thermal emission

Inside the ionized outflow: Non-thermal jet candidate

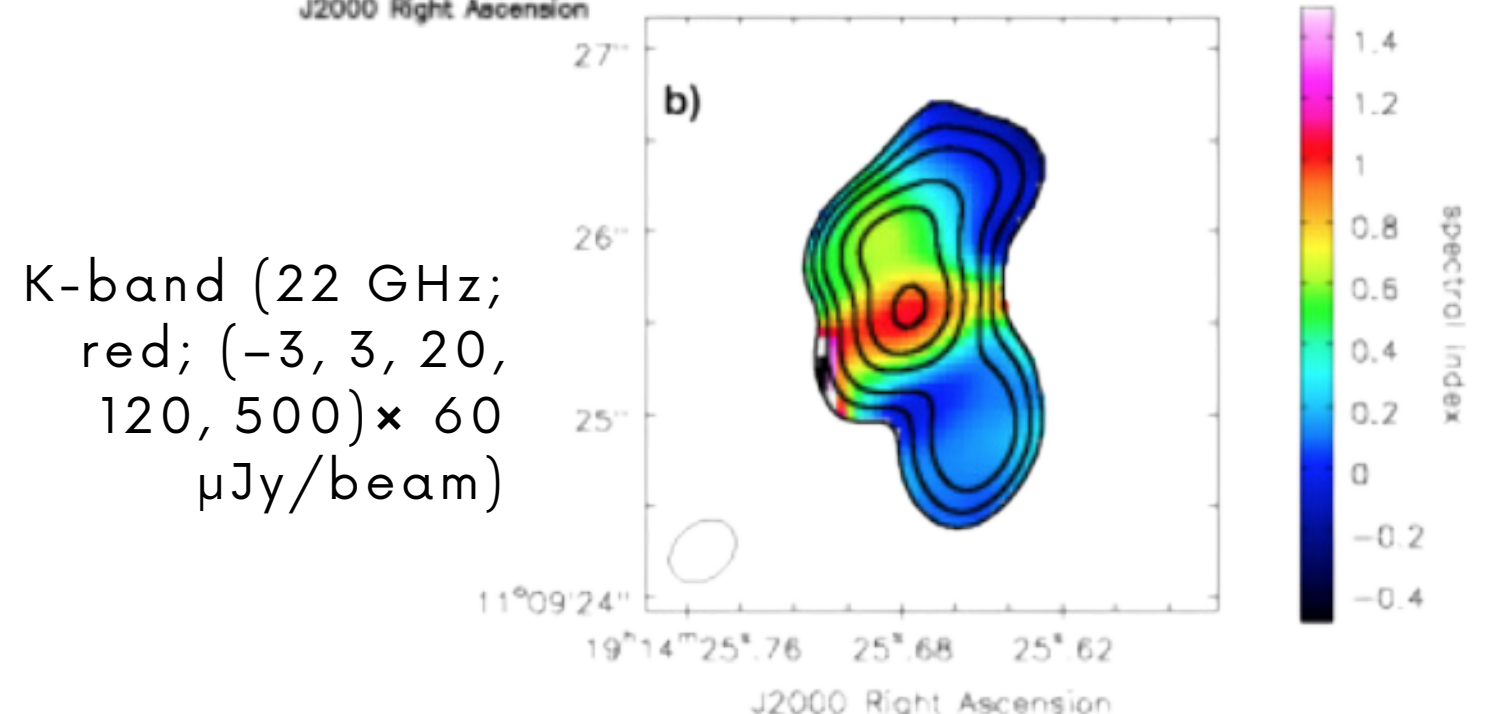
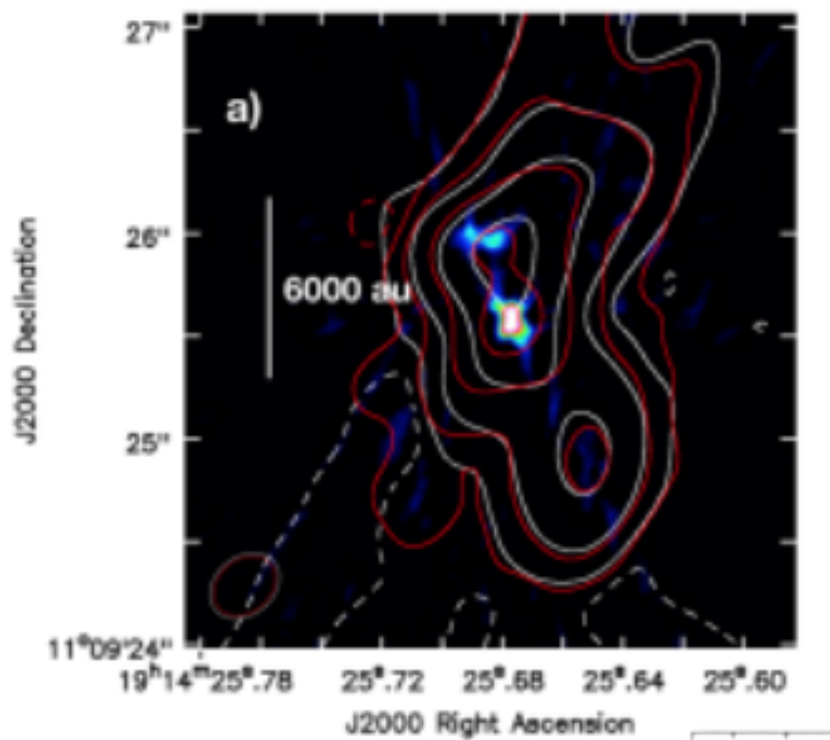
Demonstrating its presence would make G45 the first confirmed observational evidence of disk accretion

The Observations



Band	Frequency (GHz)	Central Frequency (GHz)	L (cm)
ALMA	6	211 – 275	0.13
	Q	40 – 50	0.7
	Ka	26.5-40	1
	K	18 – 26.5	1.3
	Ku	12 – 18	2
	C	4 – 8	6
VLA		234	
		44	
		33	
		22.2	
		15	
		6.7	

The Observations

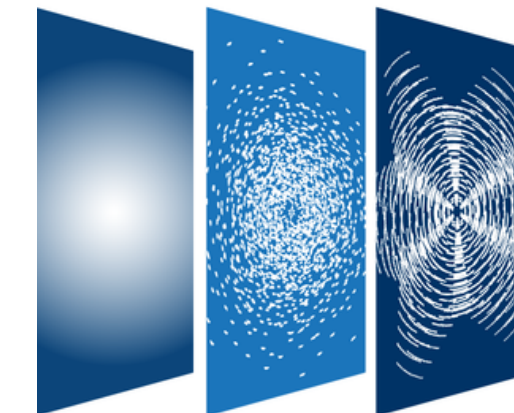
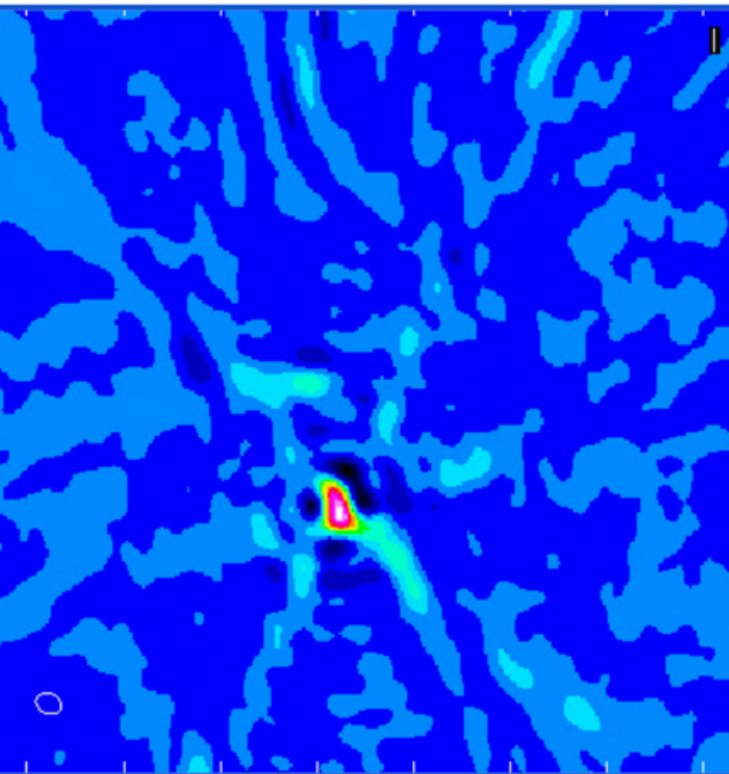
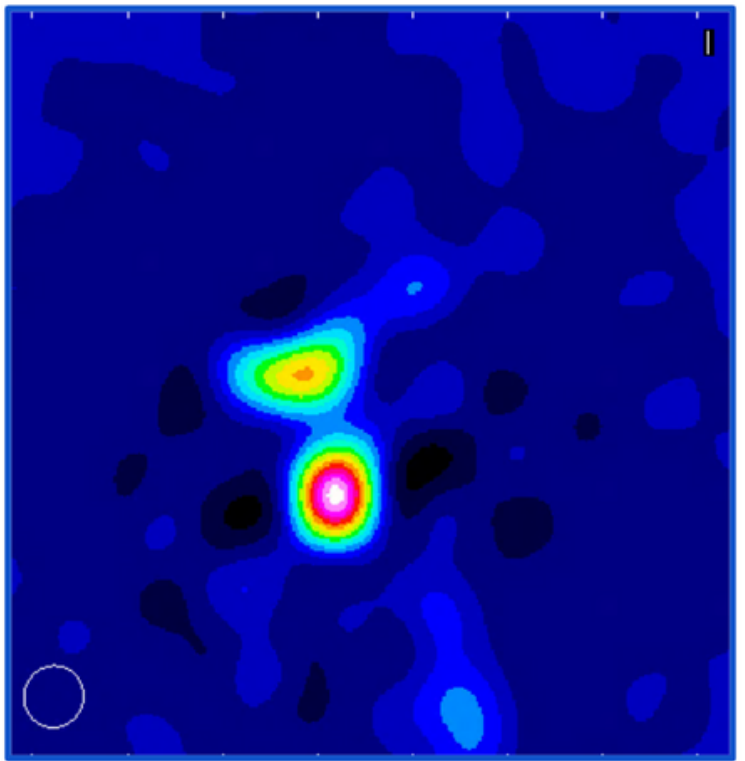


	Band	Frequency (GHz)	Central Frequency (GHz)	L (cm)	
ALMA	6	211 – 275	234	0.13	
	Q	40 – 50	44	0.7	
VLA	Ka	26.5-40	33	1	NEW!
	K	18 – 26.5	22.2	1.3	
	Ku	12 - 18	15	2	
	C	4 – 8	6.7	6	NEW!

Wide Multiband Approach!

Continuum Imaging Process

High and low resolution approach



CASA
Common Astronomy
Software Applications



Combine bands

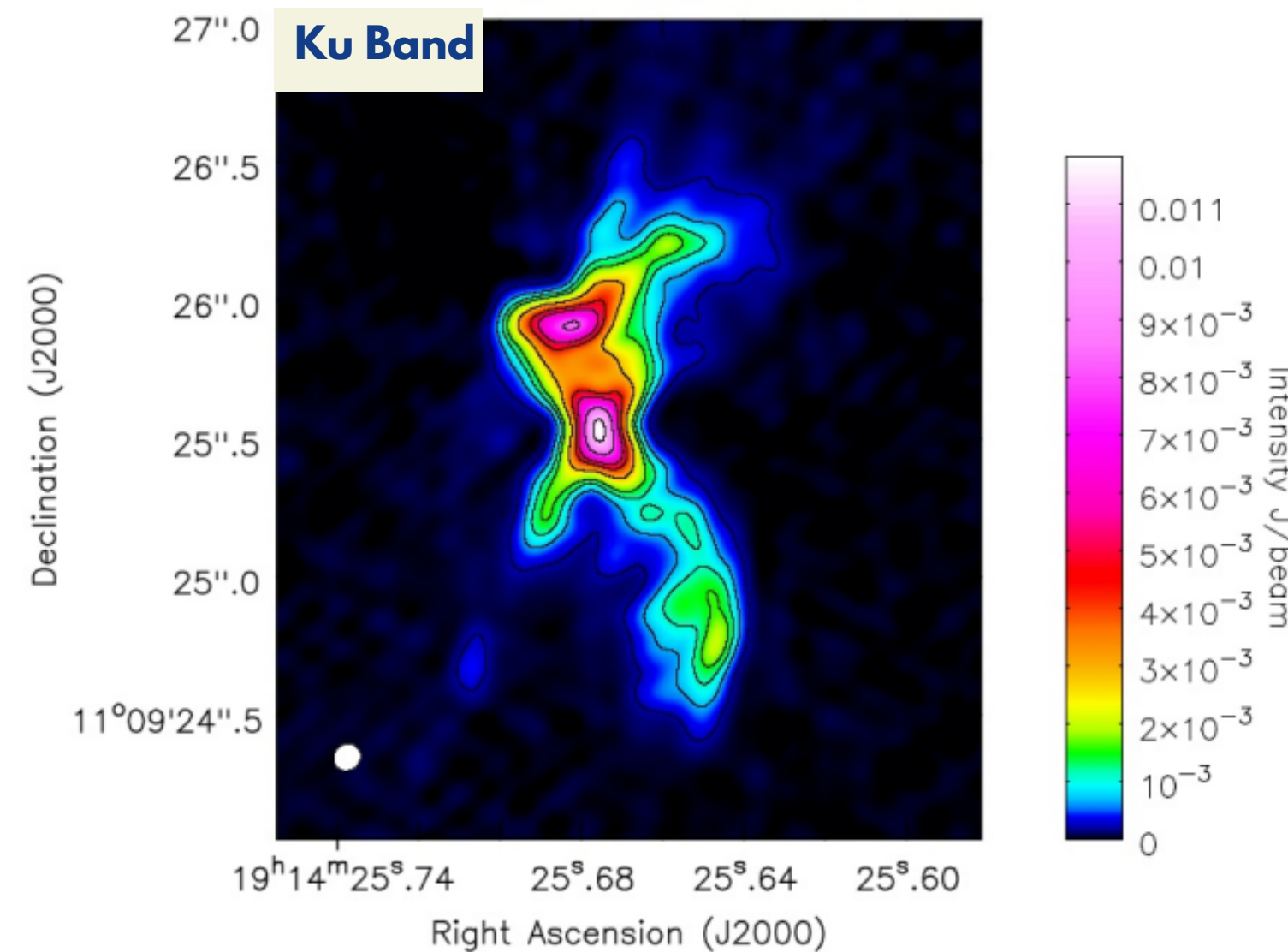
Resolve compact emissions

Enhance sensitivity without sacrificing resolution

Radio continuum results

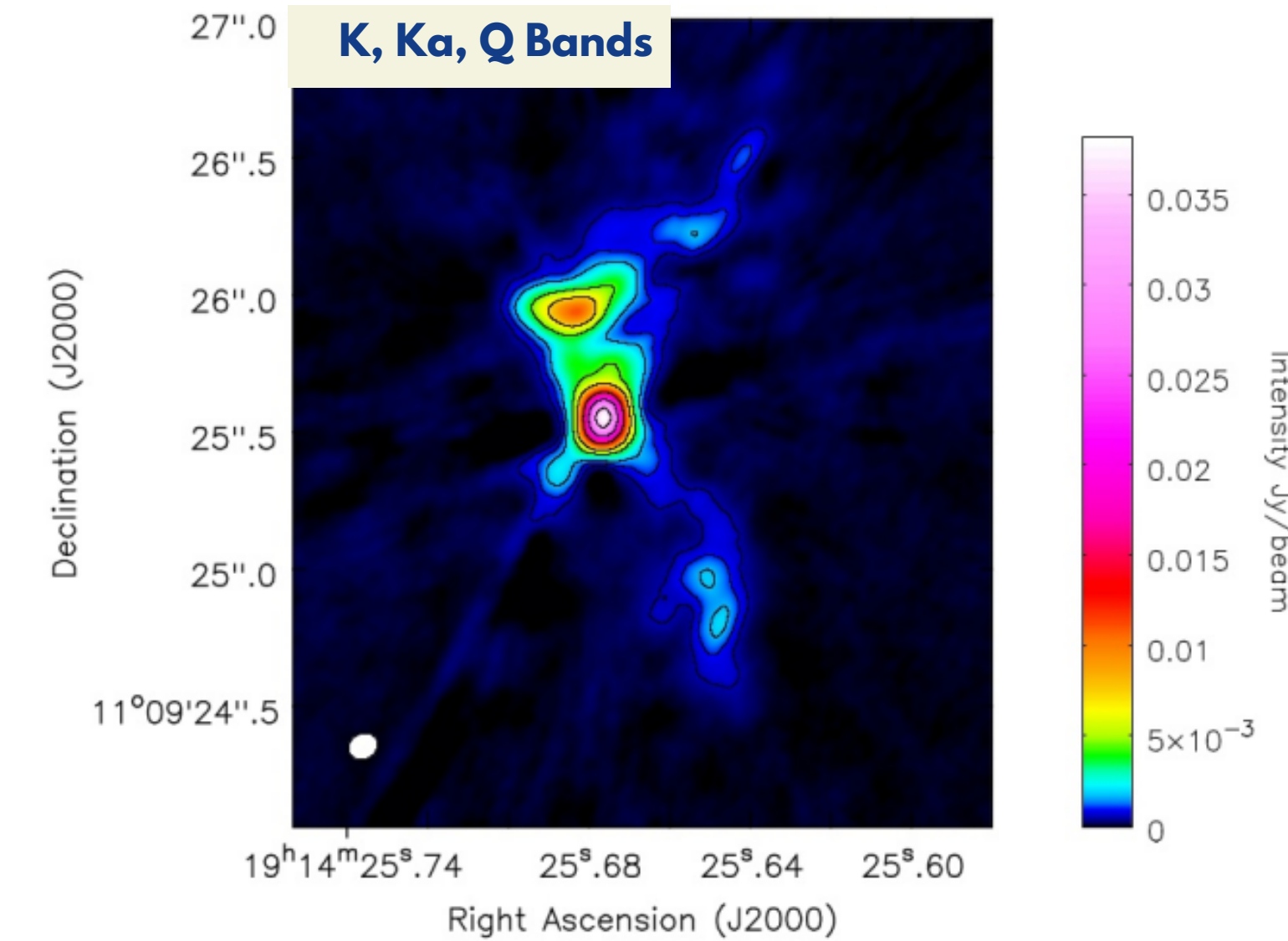
C.F 15 GHz 0.11" 0.022 mJy beam⁻¹

3 σ detection significance



$[-3, 10, 30, 50, 70, 130, 200, 250, 370, 500] \times 0.022 \text{mJy beam}^{-1}$

C.F 33.2 GHz 0.06" 0.048 mJy beam⁻¹

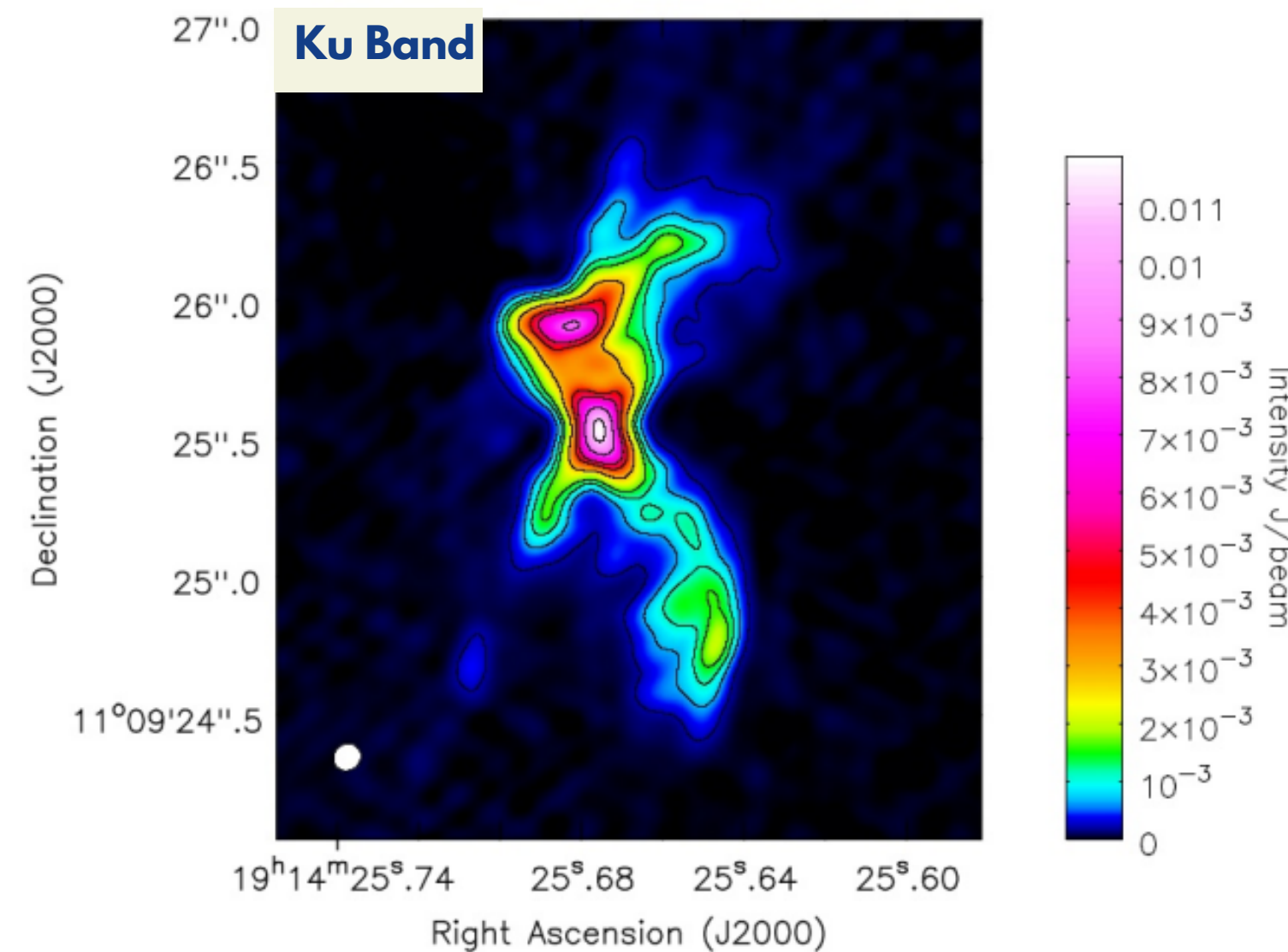


$[-3, 10, 20, 35, 90, 150, 300, 480, 700] \times 0.048 \text{mJy beam}^{-1}$

Radio continuum results

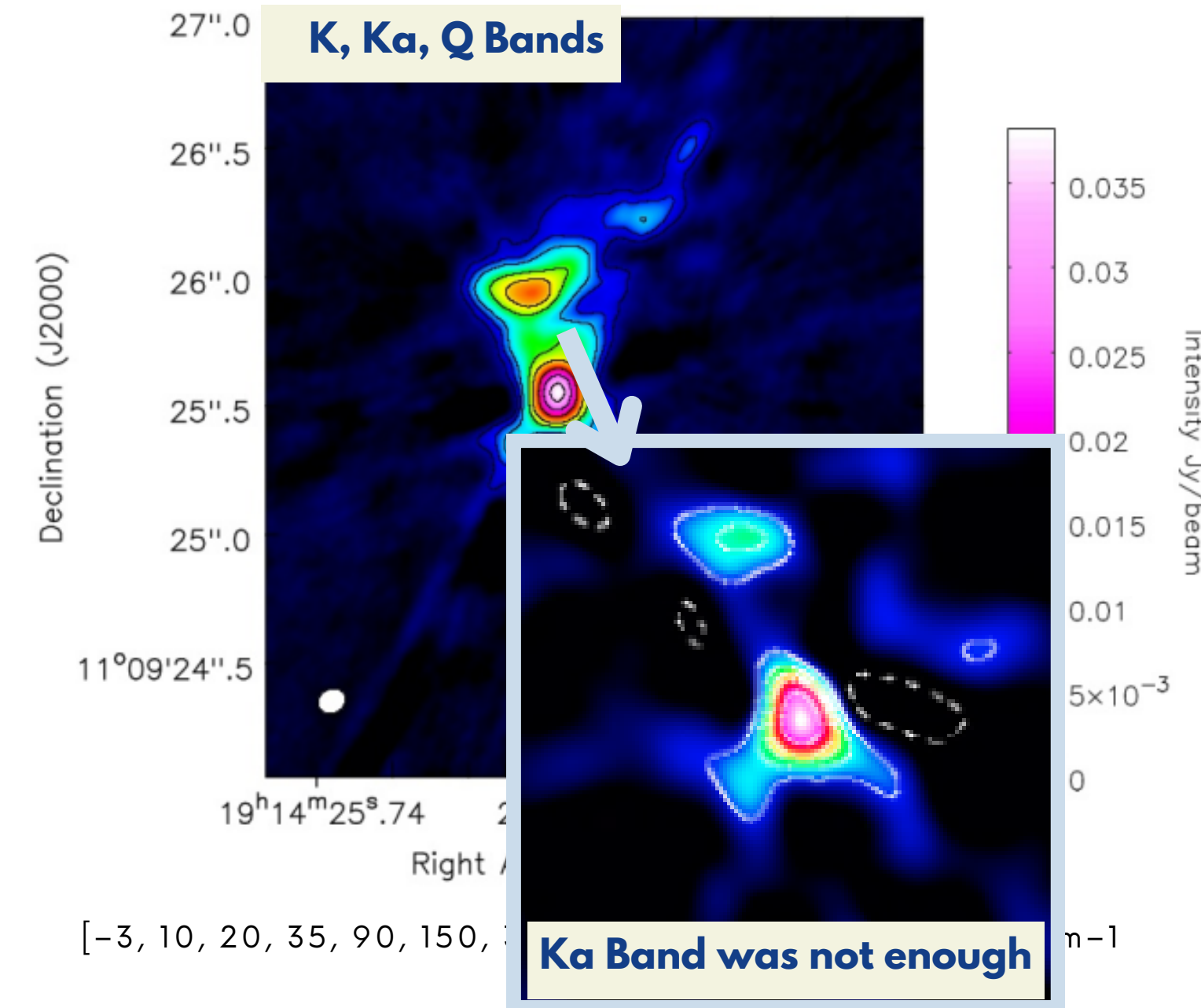
C.F 15 GHz 0.11" 0.022 mJy beam⁻¹

3 σ detection significance



$[-3, 10, 30, 50, 70, 130, 200, 250, 370, 500] \times 0.022\text{mJy beam}^{-1}$

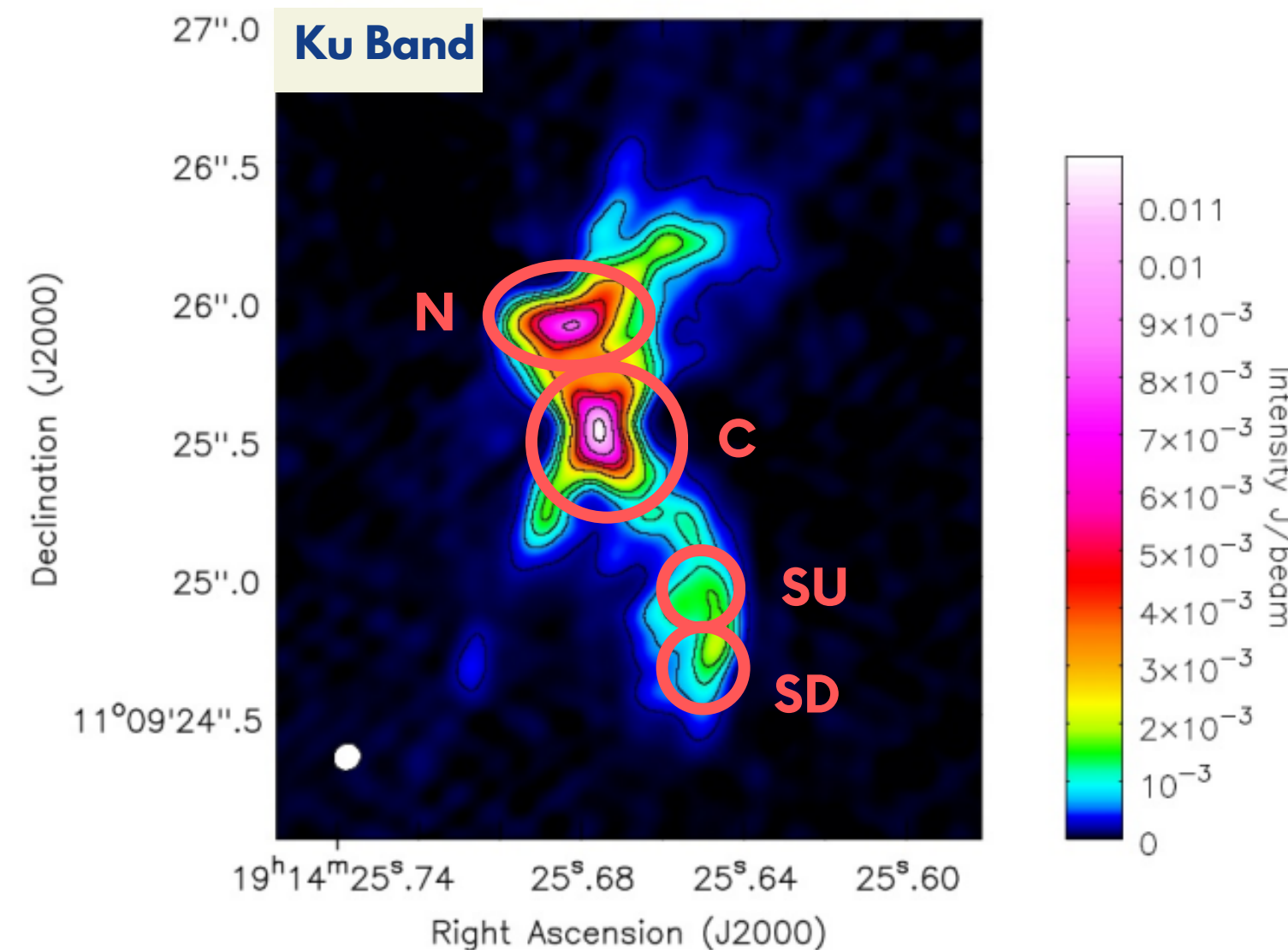
C.F 33.2 GHz 0.06" 0.048 mJy beam⁻¹



Radio continuum results

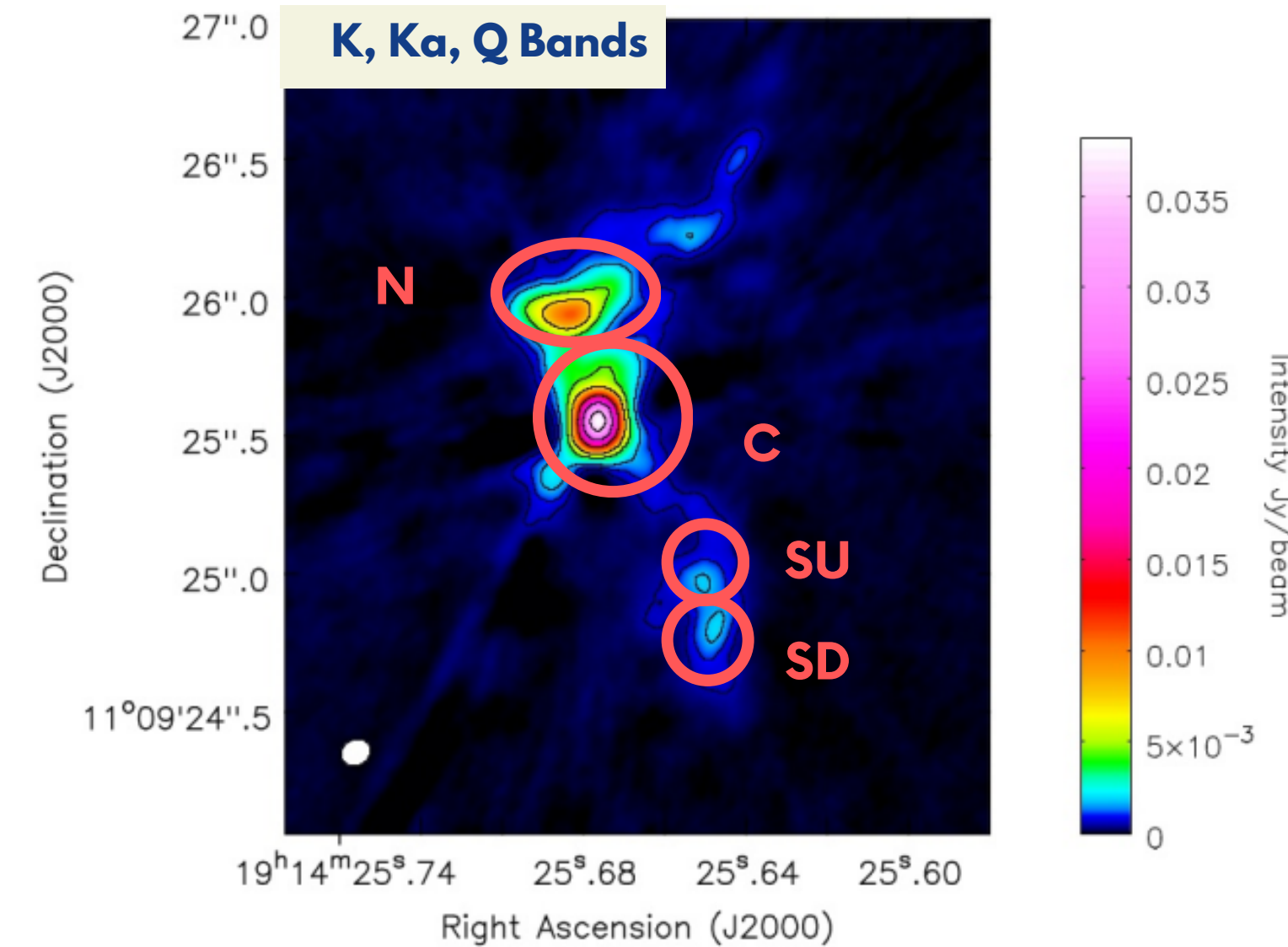
C.F 15 GHz 0.11" 0.022 mJy beam⁻¹

**How does
the
emission
change
with
frequency?**



$[-3, 10, 30, 50, 70, 130, 200, 250, 370, 500] \times 0.022 \text{mJy beam}^{-1}$

C.F 33.2 GHz 0.06" 0.048 mJy beam⁻¹



$[-3, 10, 20, 35, 90, 150, 300, 480, 700] \times 0.048 \text{mJy beam}^{-1}$

Spectral Index α

$$S(\nu) \propto \nu^\alpha$$

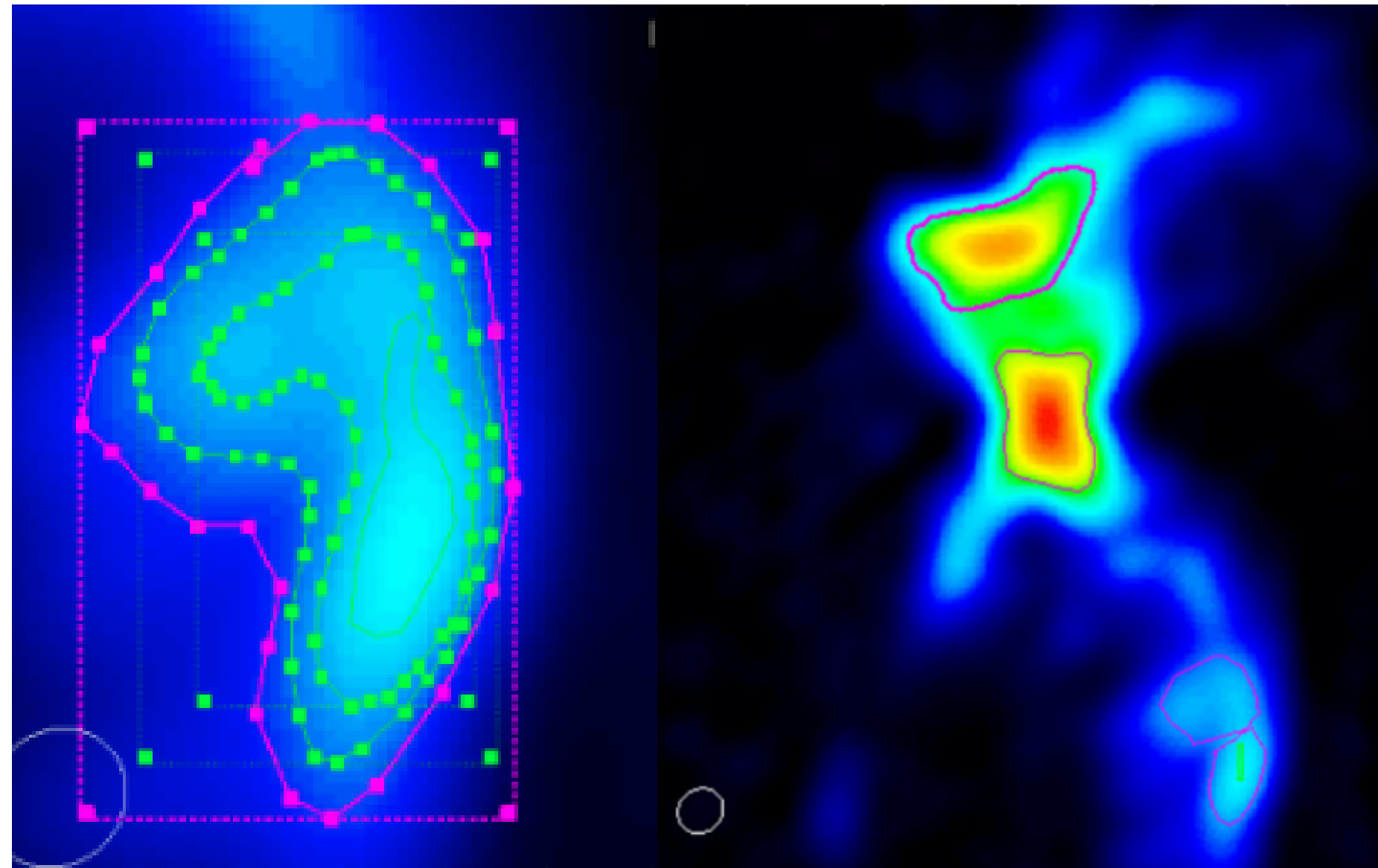
We can use this to characterize the compact emissions in the source

$$\alpha = \frac{\log\left(\frac{I_{\nu_1}}{I_{\nu_2}}\right)}{\log\left(\frac{\nu_1}{\nu_2}\right)}$$

$\nu_1 = 15 \text{ GHz}$
 $\nu_2 = 33.2 \text{ GHz}$

α Range	Emitting Source	Typical Emission Mechanism
$\alpha < 0$	Non-thermal sources	Synchrotron radiation, AGN, supernova remnants
$0 < \alpha < 1$	Ionized gas (thermal)	Free-free emission (H II regions)
$1 < \alpha < 2$	Dust (thermal)	Thermal dust emission
$\alpha \approx 2$	Very cool thermal sources	Blackbody radiation (cool stars, cold dust)
$\alpha > 2$	Very cold sources	Extremely cold dust or molecular clouds

Spectral Index α : flux extraction



imfit task could not resolve the compact sources, unreliable flux outcomes

Manual enclosing of sources based on contour levels

Same regions used on both Ku and KKaQ images

Flux densities extracted from the viewer

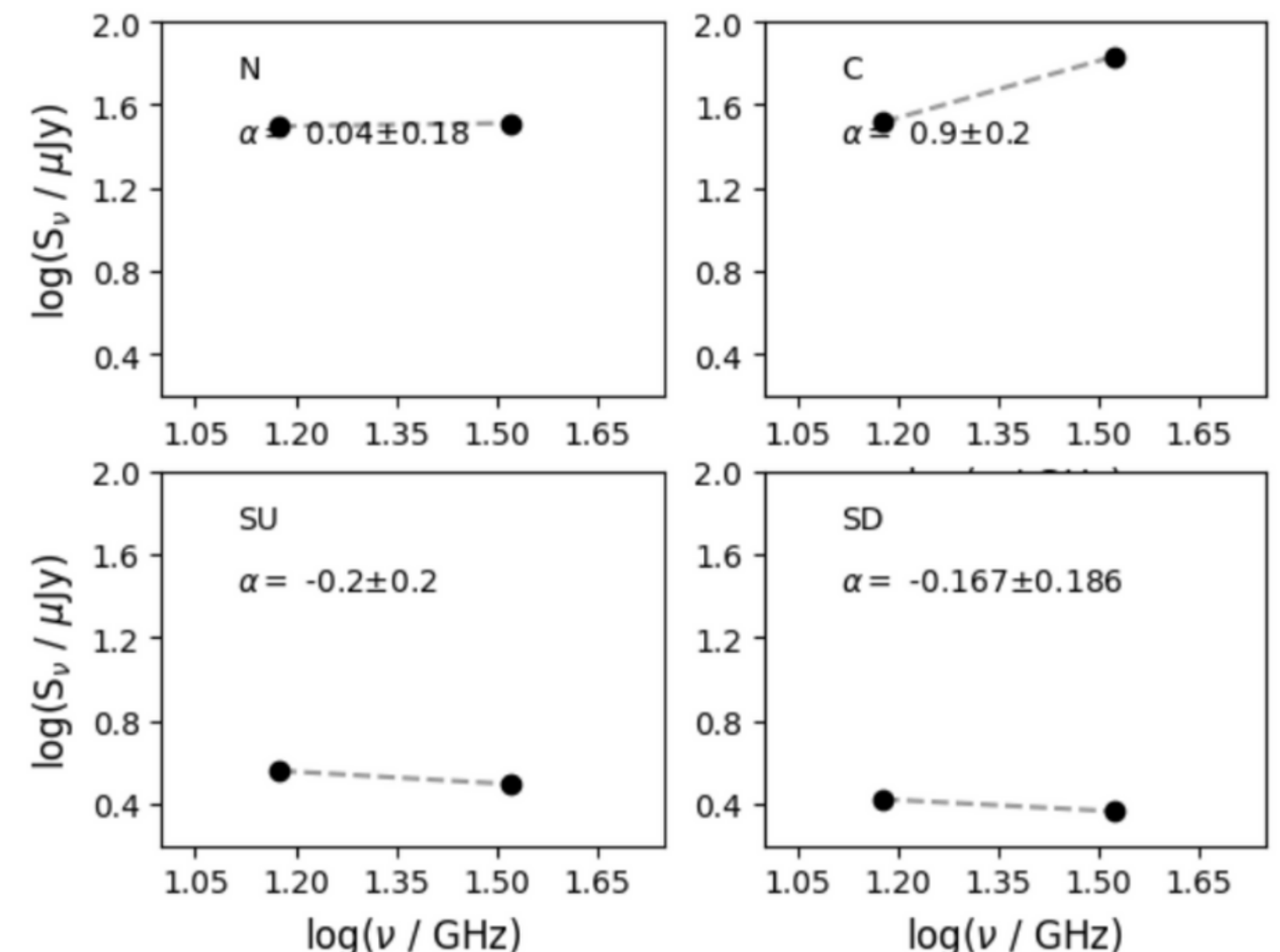
Spectral Index α : flux extraction

 $\alpha < 0$

Non-thermal sources

 $0 < \alpha < 1$

Ionized gas (thermal)



Source	R.A. (J2000)	Decl. (J2000)	Size (" × ")	$S_{\nu 15GHz}$ (mJy)	$S_{\nu 33.2GHz}$ (mJy)	α
G45N	19:14:25.682	11.09.25.986	0.4 × 0.22	31.40 ± 0.06	32.50 ± 0.12	0.04 ± 0.18
G45C	19:14:25.676	11.09.25.552	0.28 × 0.18	32.80 ± 0.05	67.80 ± 0.10	0.90 ± 0.2
G45SU	19:14:25.650	11.09.24.969	0.20 × 0.19	3.63 ± 0.04	3.13 ± 0.08	-0.2 ± 0.2
G45SD	19:14:25.648	11.09.24.804	0.19 × 0.11	2.65 ± 0.03	2.32 ± 0.06	-0.17 ± 0.18

Flux density uncertainty

$$\sigma_{S_\nu} = \sigma_{\text{image}} \times \left(\frac{\text{npts}}{\text{beam area}} \right)^{0.5}$$

Added in quadrature with an assumed 10% error in calibration

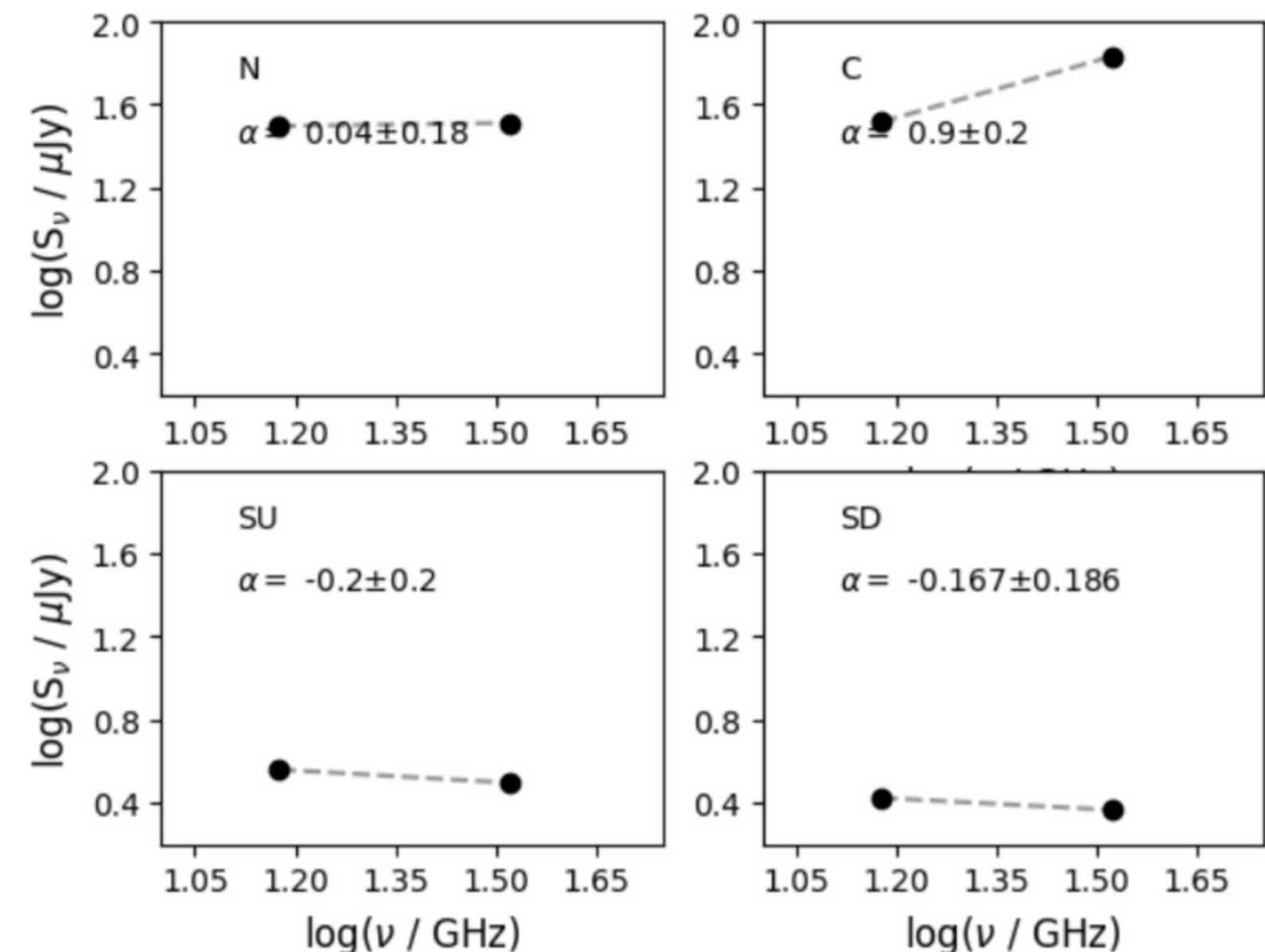
Spectral Index α : flux extraction

 $\alpha < 0$

Non-thermal sources

 $0 < \alpha < 1$

Ionized gas (thermal)



Source	R.A. (J2000)	Decl. (J2000)	Size ("' × '')	$S_{\nu 15\text{GHz}} (\text{mJy})$	$S_{\nu 33.2\text{GHz}} (\text{mJy})$	α
G45N	19:14:25.682	11.09.25.986	0.4 × 0.22	31.40 ± 0.06	32.50 ± 0.12	0.04 ± 0.18
G45C	19:14:25.676	11.09.25.552	0.28 × 0.18	32.80 ± 0.05	67.80 ± 0.10	0.90 ± 0.2
G45SU	19:14:25.650	11.09.24.969	0.20 × 0.19	3.63 ± 0.04	3.13 ± 0.08	-0.2 ± 0.2
G45SD	19:14:25.648	11.09.24.804	0.19 × 0.11	2.65 ± 0.03	2.32 ± 0.06	-0.17 ± 0.18

Source	α
G45N	0.04 ± 0.18
G45C	0.90 ± 0.2
G45SU	-0.2 ± 0.2
G45SD	-0.17 ± 0.18

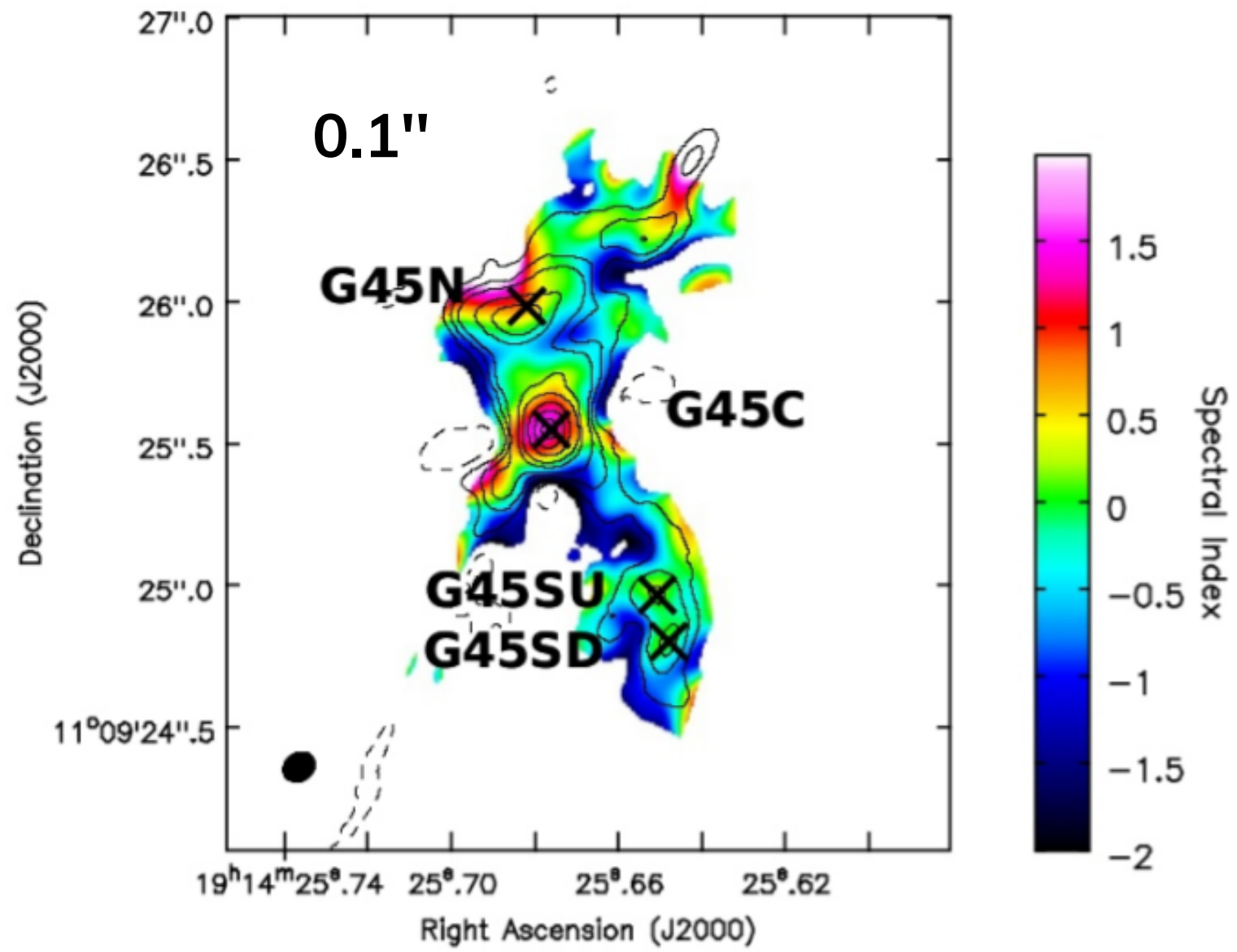
Agrees with initial characterization by Zhang et al. 2019

Not conclusive enough

Spectral Index α : mapping

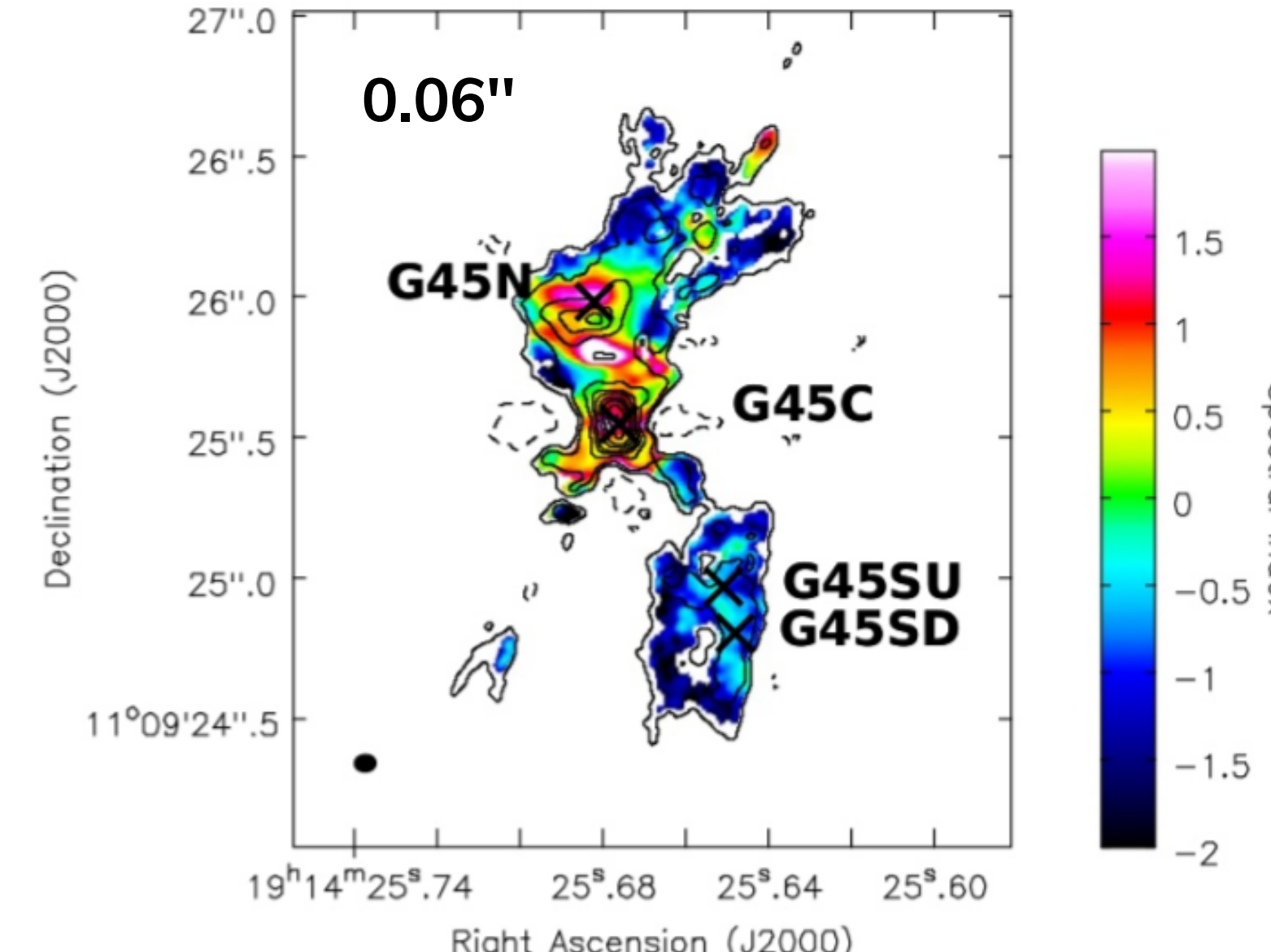
Pixel-by-pixel map
Ku Band - KKaQ Image

12-50 GHz 0.048 mJy beam⁻¹



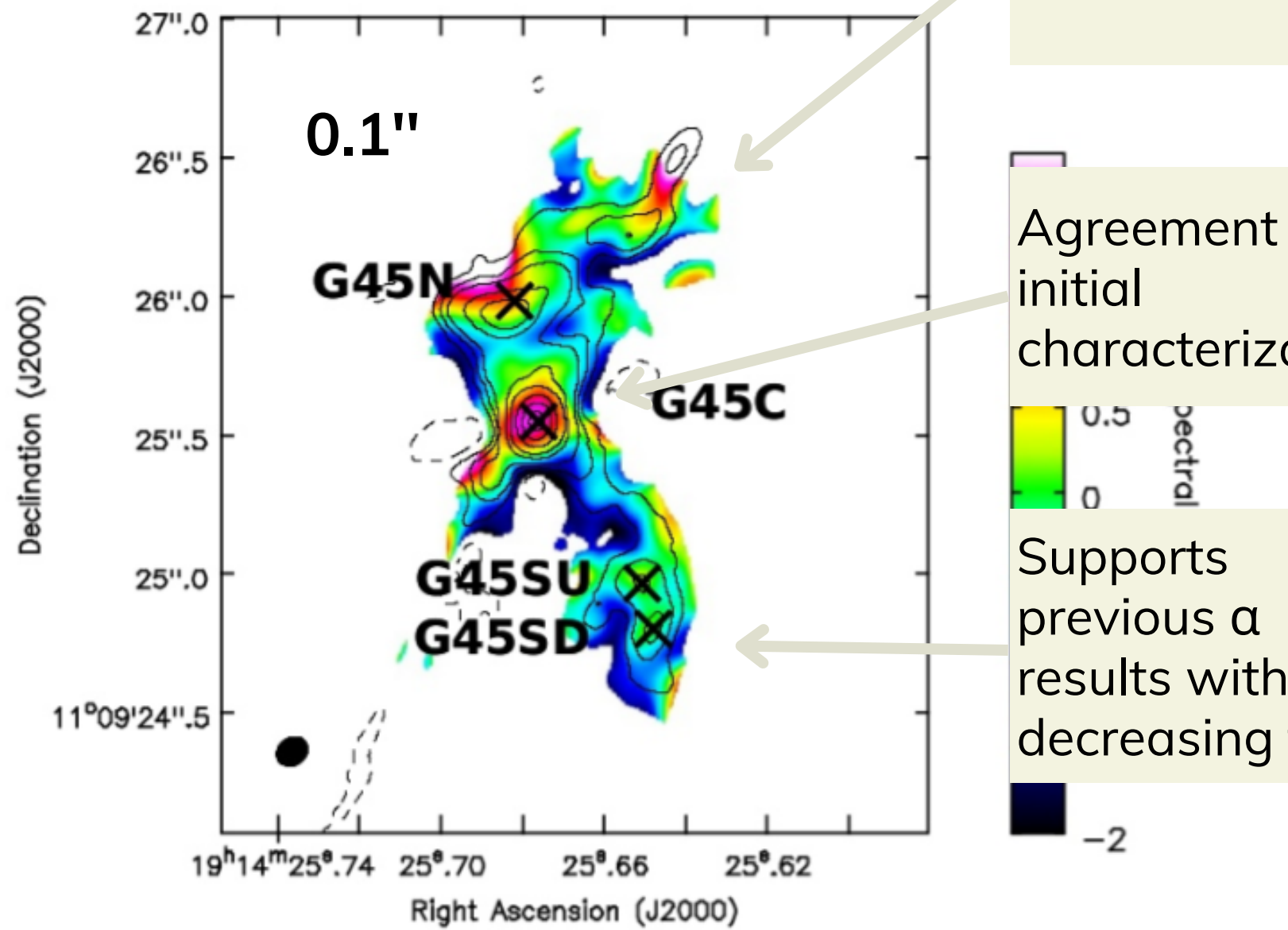
In-band wideband map
CKuKKaQ Bands

4-50 GHz 0.048 mJy beam⁻¹



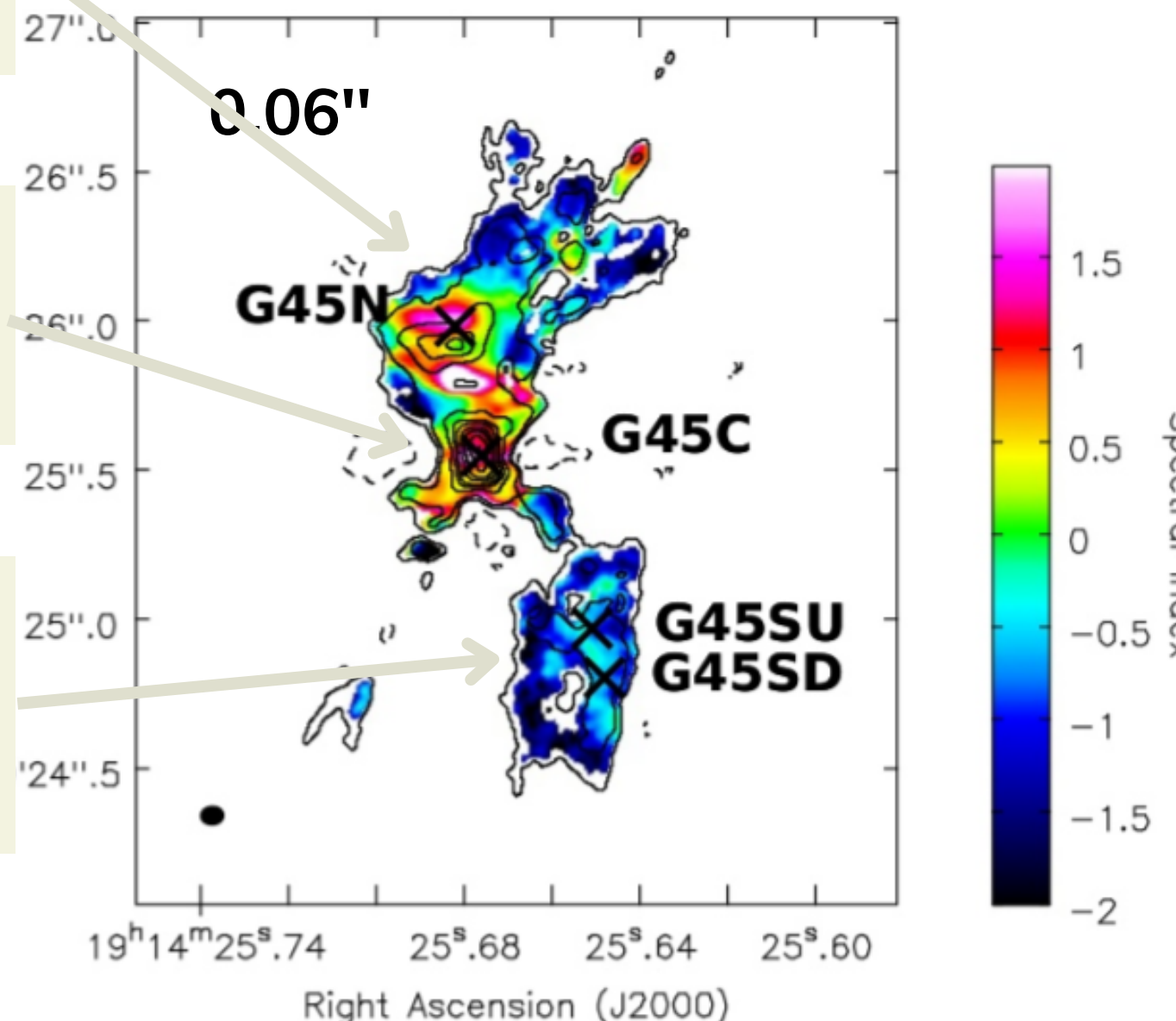
Spectral Index α : mapping

Pixel-by-pixel map
Ku Band - KKaQ Image
12-50 GHz 0.048 mJy beam $^{-1}$

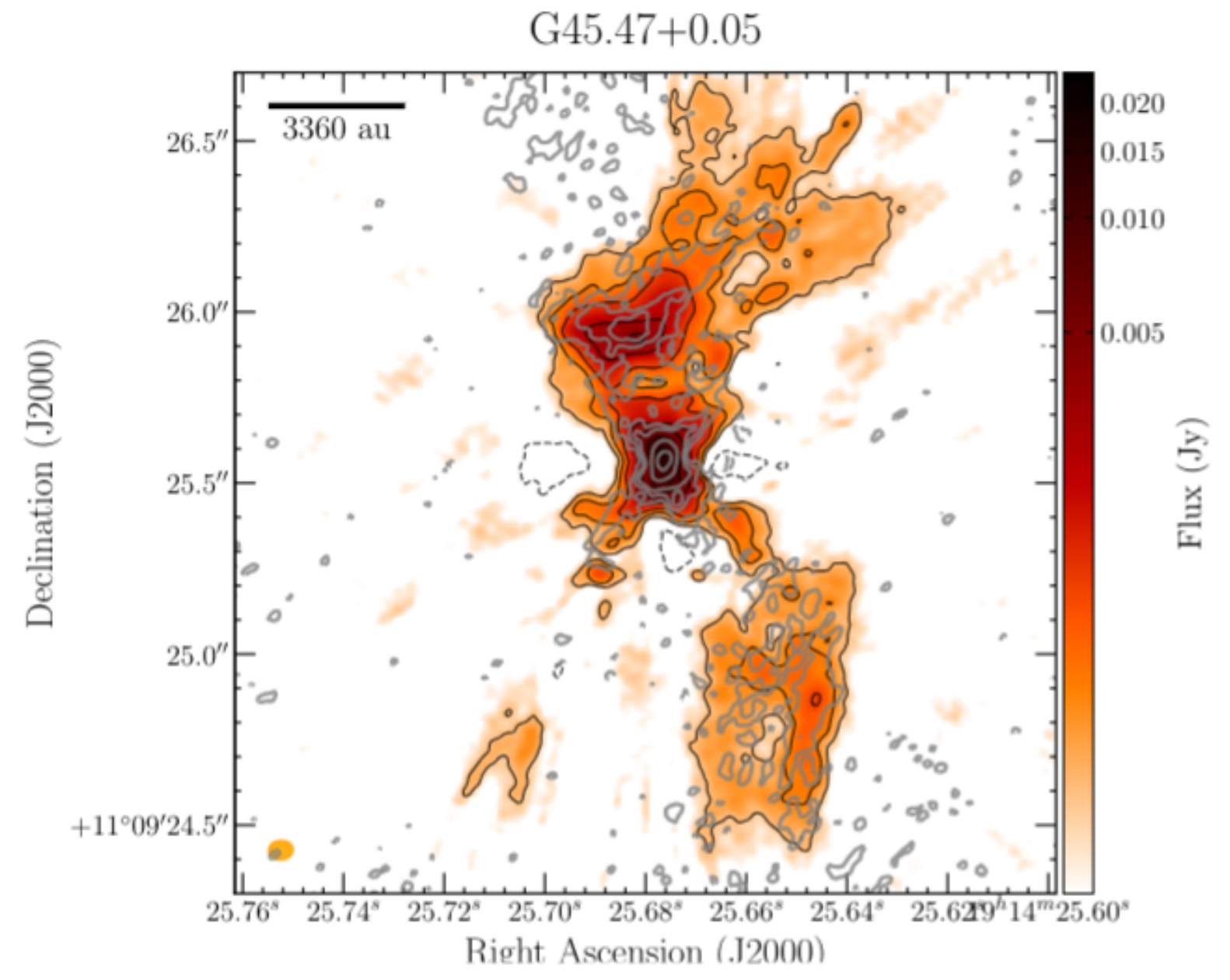


Steep values to the north
Agreement with initial characterization
Supports previous α results with a decreasing trend

In-band wideband map
CKuKKaQ Bands
4-50 GHz 0.022 mJy beam $^{-1}$



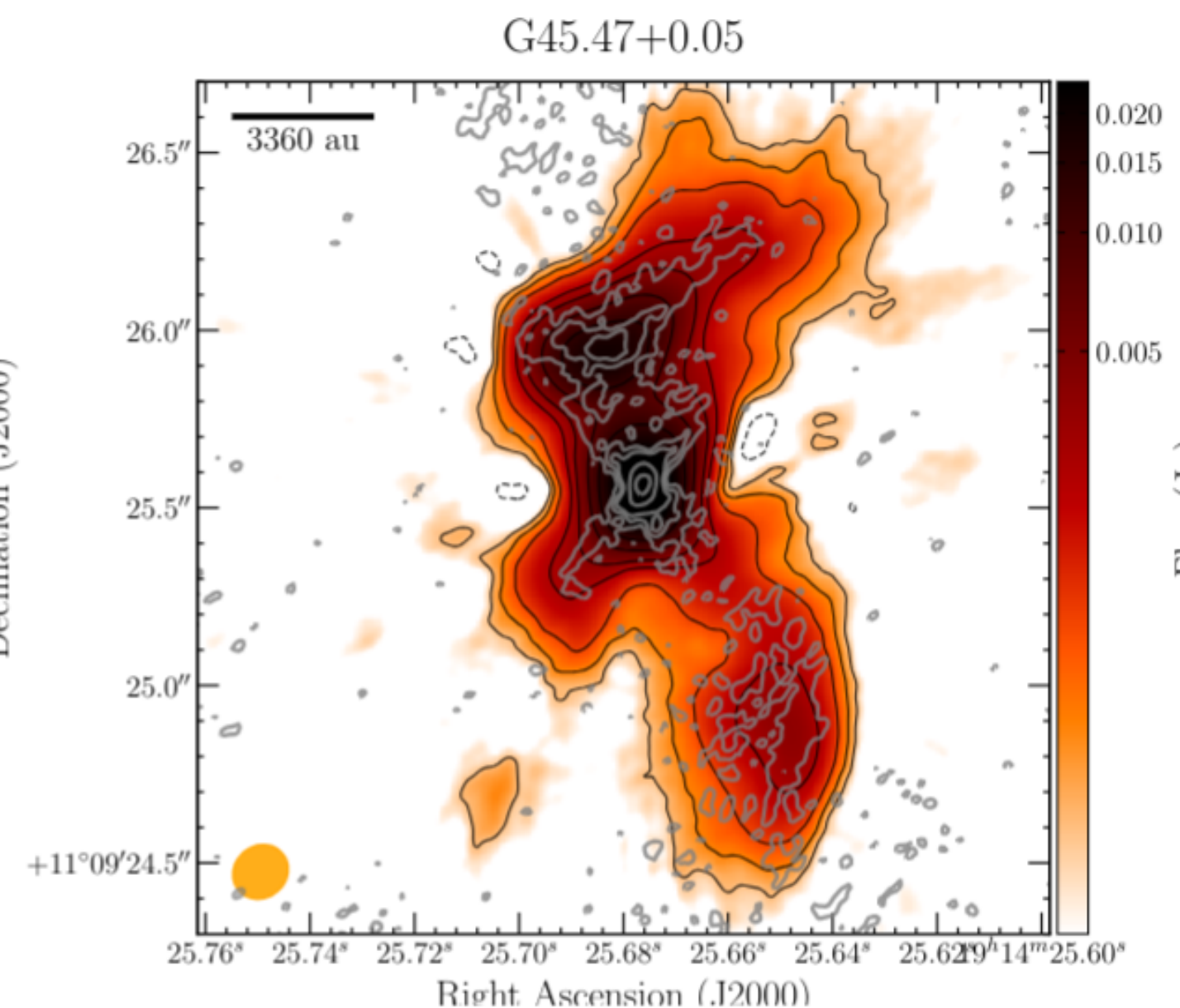
ALMA vs VLA



VLA 0.06''

ALMA 0.03''

ALMA 1.3 mm [-5, 3, 10, 20, 200, 1000] $\times 0.047\text{mJy beam}^{-1}$ grey contours
Compare mm dust emission with submm ionization



VLA 0.1''

ALMA 0.03''

Possible scenarios

Photoionized Dust Clumps

Dense Material Hosting an Embedded Jet



FACoM
Grupo de
Física y Astrofísica
Computacional
Instituto de Física - Universidad de Antioquia

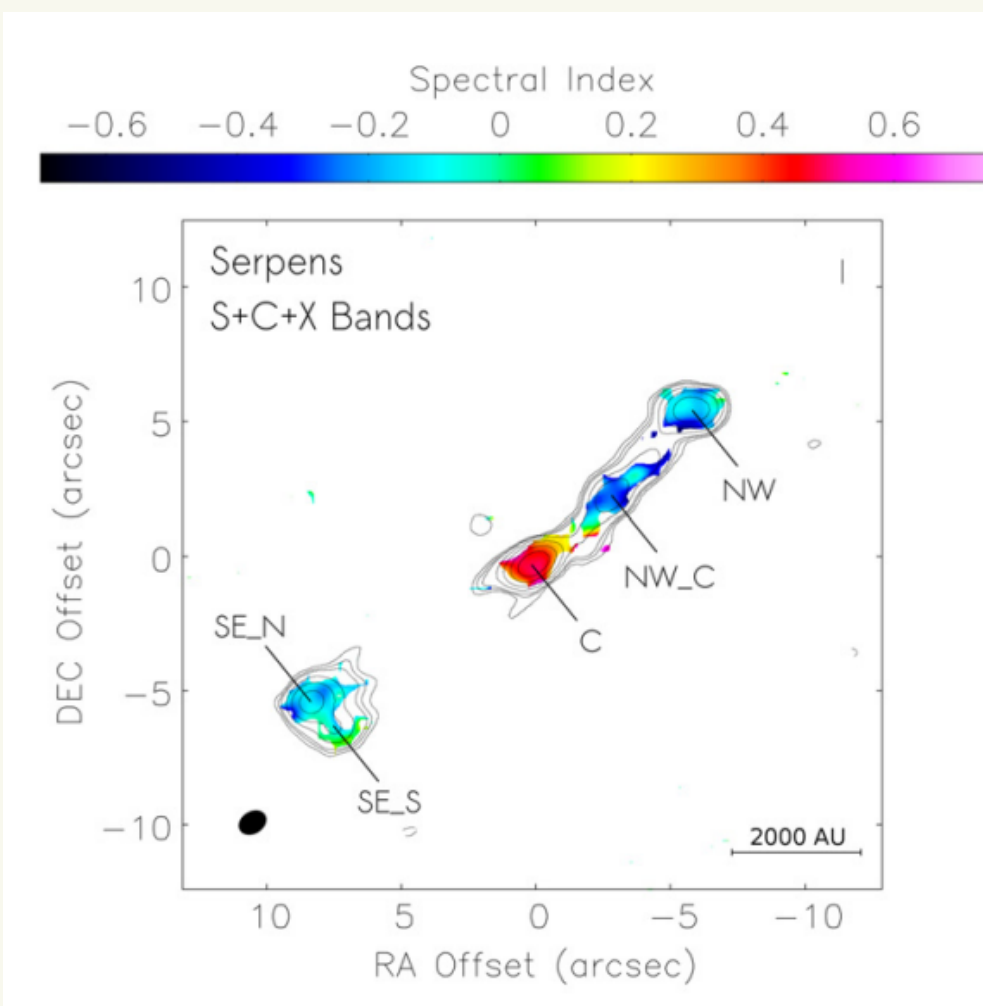
21

Presented by: Ana Sofía Marulanda-Duque
sofia.marulanda2@udea.edu.co

Possible scenarios

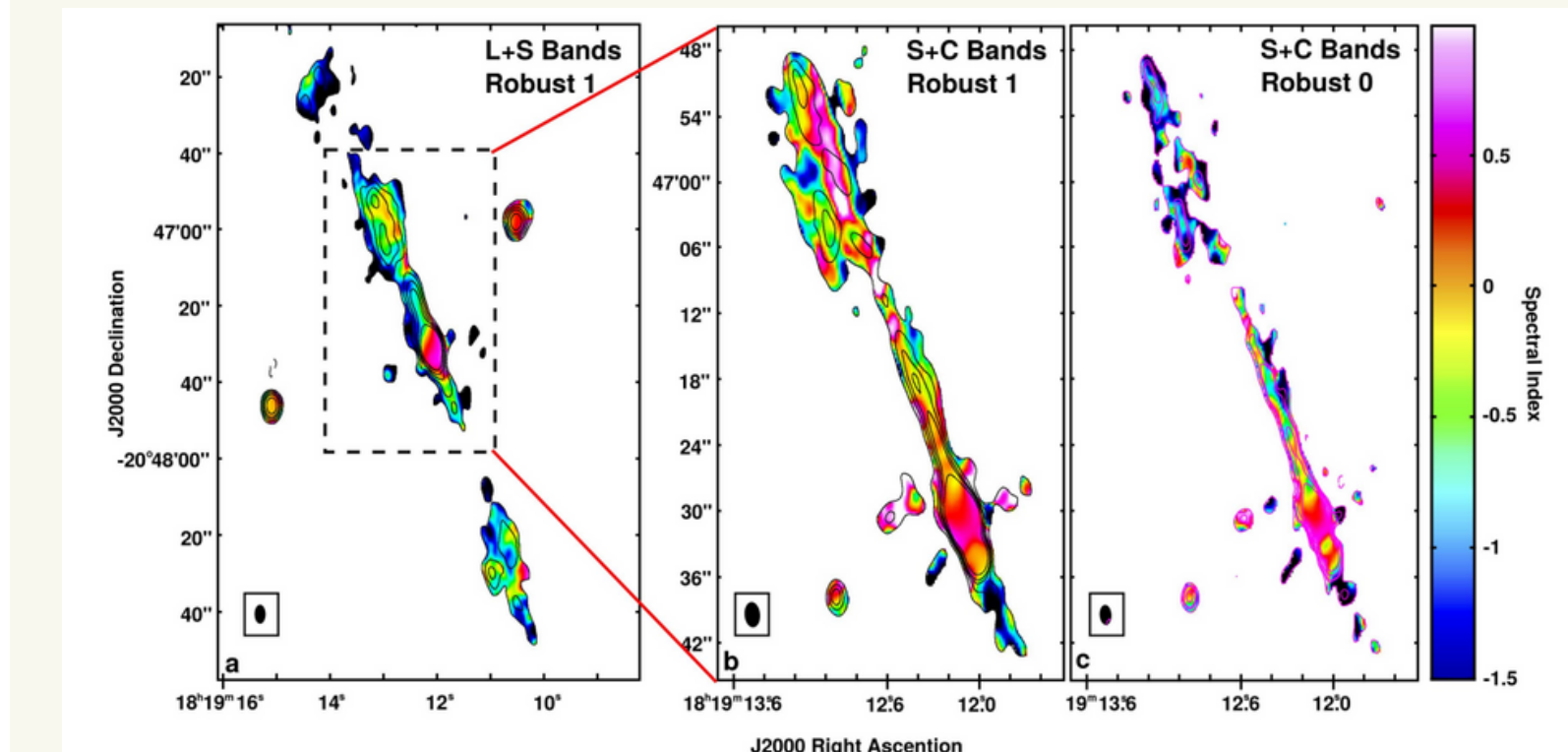
Photoionized Dust Clumps

Dense Material Hosting an Embedded Jet



Triple source in serpens

Intermediate mass source
Direct observation



HH 80-81

Detection of linearly polarized radio emission

Possible scenarios

Photoionized Dust Clumps

Dense Material Hosting an Embedded Jet

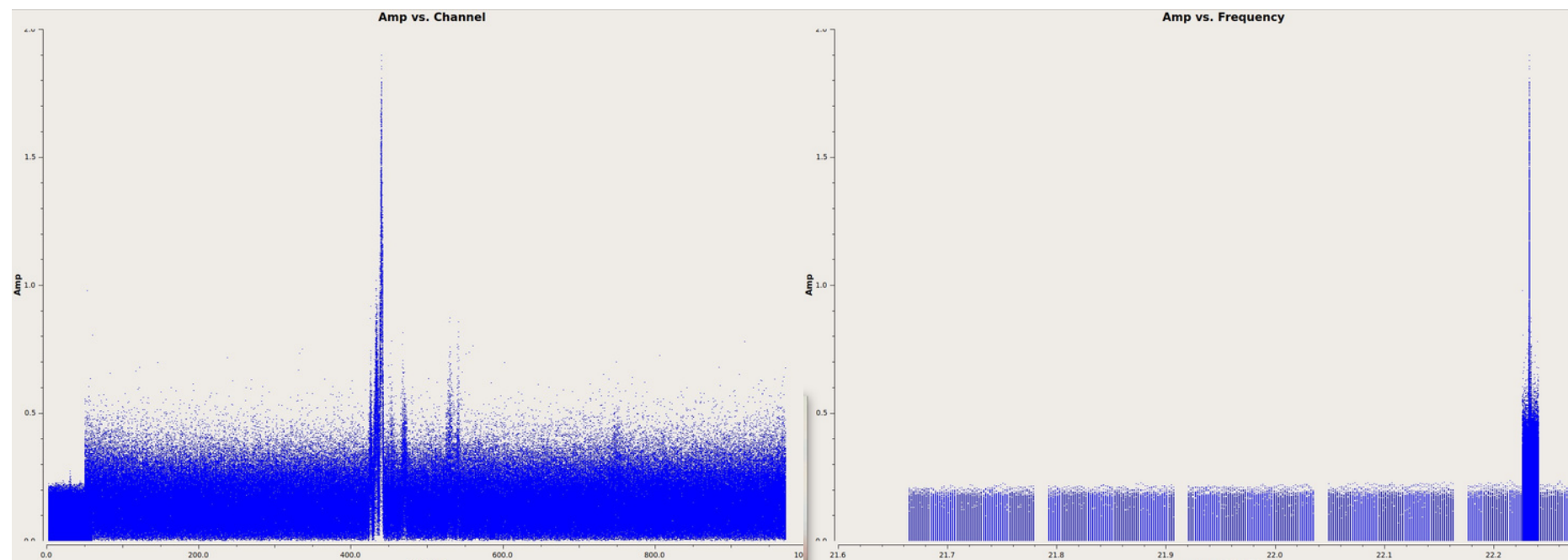
22 GHz Water Maser

K Band

Bandwith 18 – 26.5

C.F 22.2

I (cm) 1.3



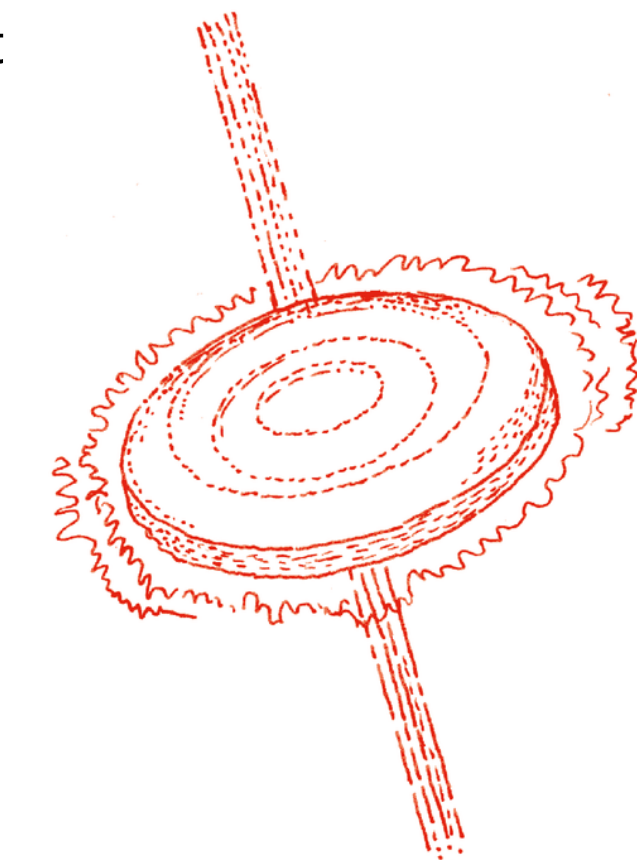
Proper Motion

Relative velocity of the jet

0.06'' resolution

Observational proposal

$$V_{\text{PM}}(\text{km s}^{-1}) = 4.74 D_{\text{kpc}} \text{ PM}(\text{mas yr}^{-1}),$$



Conclusions

Conclusions

Weak emission is detected on the southern lobe and isolated from upper sources

The wideband image (4-50 GHz) significantly improved the sensitivity

Although the nature of the emission from the region cannot be conclusively determined, we have restricted the emission from the candidate jet to two possible scenarios that align with large-scale structures and the evolutionary phase indicated by the feedback effects of the sources.

THANK YOU!

Thanks to



FACoM
Grupo de
Física y Astrofísica
Computacional
Instituto de Física - Universidad de Antioquia

26

Presented by: Ana Sofía Marulanda-Duque
sofia.marulanda2@udea.edu.co

THANK YOU!

Thanks to

Viviana Rosero (Caltech)

Joshua Marvil (NRAO)

Kei Tanaka (Tokio Tech)

Yichen Zhang (University of Virginia)

Germán Chaparro (Universidad de Antioquia)

Red de Estudiantes Colombianos de Astronomía

National Radio Astronomy Observatory

Grupo de Física y Astrofísica Observacional UdeA



Grupo de
Física y Astrofísica
Computacional
Instituto de Física - Universidad de Antioquia

27

Presented by: Ana Sofía Marulanda-Duque
sofia.marulanda2@udea.edu.co

- De Buizer, J. M., Liu, M., Tan, J. C., et al. 2017, *The Astrophysical Journal*, 843, 33, doi: 10.3847/1538-4357/aa74c8
- Urquhart, J. S., Hoare, M. G., Purcell, C. R., et al. 2009, *Astronomy & Astrophysics*, 501, 539, doi: 10.1051/0004-6361/200912108
- Ortega, M. E., Paron, S., Cichowski, S., Rubio, M., & Dubner, G. 2012, *Astronomy & Astrophysics*, 546, A96, doi: 10.1051/0004-6361/201219424
- Tanaka, K. E. I., Tan, J. C., & Zhang, Y. 2016, *The Astrophysical Journal*, 818, 52, doi: 10.3847/0004-637X/818/1/5
- Zhang, Y., Tan, J. C., Sakai, N., et al. 2019a, *The Astrophysical Journal*, 873, 73, doi: 10.3847/1538-4357/ab0553
- Zhang, Y., Tanaka, K. E. I., Rosero, V., et al. 2019b, *The Astrophysical Journal Letters*, 886, L4, doi: 10.3847/2041-8213/ab5309
- Rodríguez-Kamenetzky, A., Carrasco-González, C., Araudo, A., et al. 2016, *The Astrophysical Journal*, 818, 27, doi: 10.3847/0004-637X/818/1/27
- Rosero, V., Tanaka, K. E. I., Tan, J. C., et al. 2019, *The Astrophysical Journal*, 873, 20, doi: 10.3847/1538-4357/ab0209
- Cesaroni, R., Olmi, L., Walmsley, C. M., Churchwell, E., & Hofner, P. 1994, *The Astrophysical Journal*, 435, L137, doi: 10.1086/187613

References